Higgs boson property measurements (mass, width, CP) in ATLAS

Elise Le Boulicaut Ennis (Yale), on behalf of the ATLAS Collaboration

Higgs Hunting 2025 [indico]

July 15, 2025

Introduction

- Studying **Higgs boson properties** is essential for probing the Standard Model (SM) with high precision.
- Any **deviations** from expectations could be signs of new physics.
- Some Beyond the SM (BSM) theories predict effects on the **mass, width, and Charge-Parity (CP)** of the Higgs boson.

- Will highlight the most recent ATLAS results on Higgs mass, width, and CP.

Mass measurement

• • •

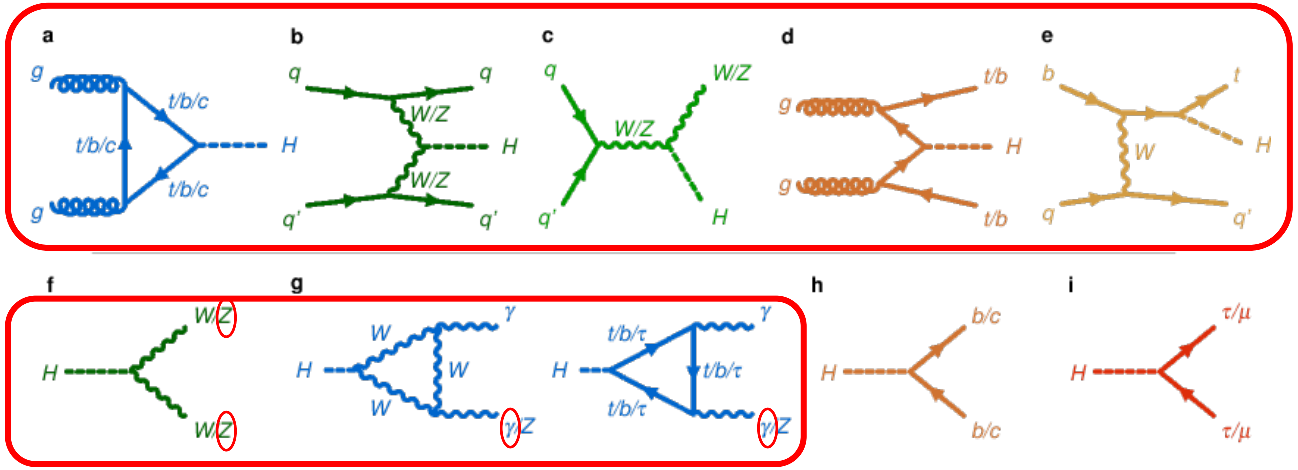

https://cds.cern.ch/record/2814946/plots

Introduction

- Higgs mass (m_H) not predicted in the SM.
- Necessary **input** to calculate other parameters (e.g. couplings).
- Related to the **stability** of the Electro-Weak vacuum.

- $H \rightarrow \gamma\gamma$ and $H \rightarrow ZZ^* \rightarrow 4\ell$ chosen for their good **resolution**.

Mass measurement in $H \rightarrow \gamma\gamma$

Latest result from 2023: Phys. Lett. B **847** (2023) 138315 using full Run 2 (140 fb^{-1})

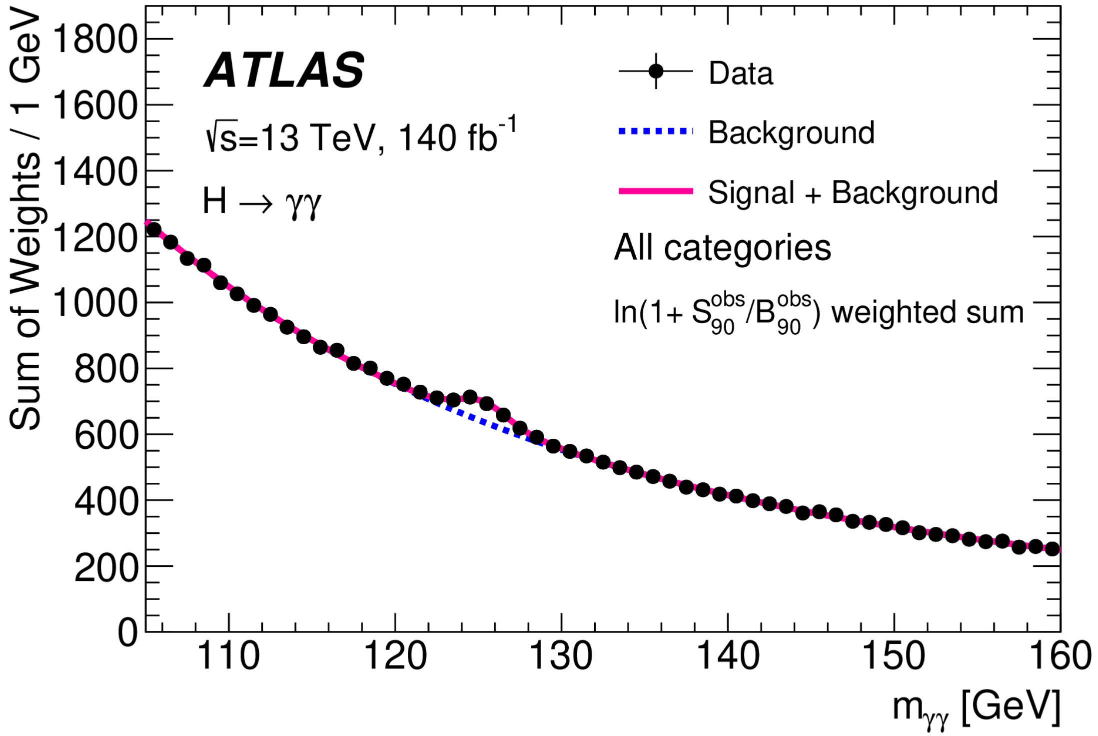

Mass measurement in $H \to \gamma\gamma$

Latest result from 2023: [Phys. Lett. B **847** (2023) 138315]() using full Run 2 (140 fb^{-1})

Signal = double-sided Crystal Ball function

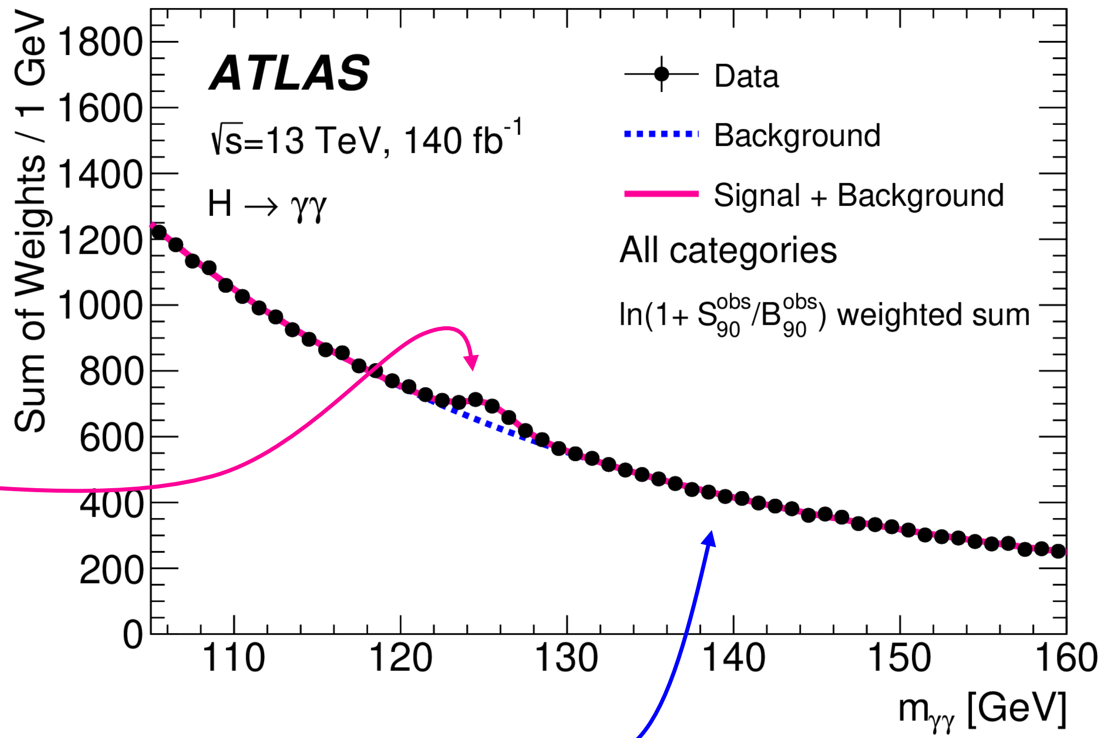

Background = empirical continuous function of $m_{\gamma\gamma}$, fit in sidebands and extrapolated to Higgs peak region

Mass measurement in $H \to \gamma\gamma$

Latest result from 2023: [Phys. Lett. B **847** (2023) 138315] using full Run 2 (140 fb^{-1})

Signal = double-sided Crystal Ball function

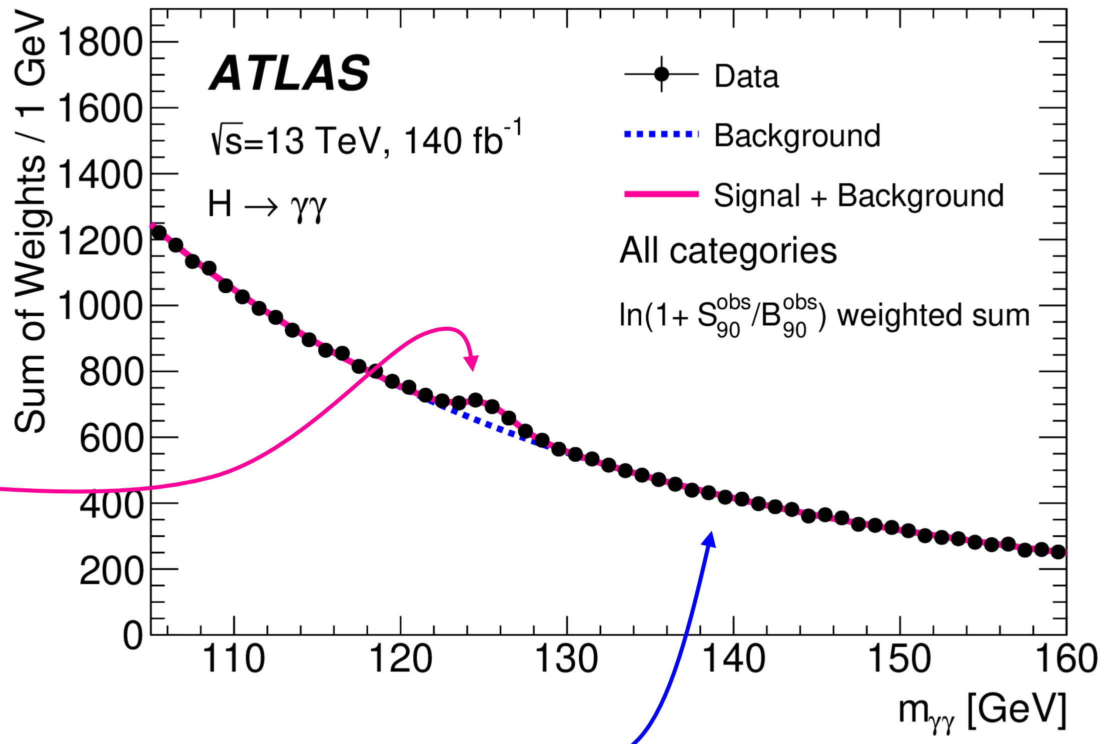

Background = empirical continuous function of $m_{\gamma\gamma}$, fit in sidebands and extrapolated to Higgs peak region

Improvements with respect to [partial Run 2 result]:

- Classification into 14 categories, optimized specifically to minimize uncertainty on m_H → **6% reduction** (considering statistics and photon energy scale uncertainties only).
- Improved photon reconstruction.
- New auxiliary measurement to constrain E_T-dependent electron energy scale → **factor of 4 reduction** in photon energy scale/resolution uncertainty.

Mass measurement in $H \rightarrow ZZ^* \rightarrow 4\ell$

Latest result from 2023: Phys. Lett. B **843** (2023) 137880 using full Run 2 (139 fb^{-1})

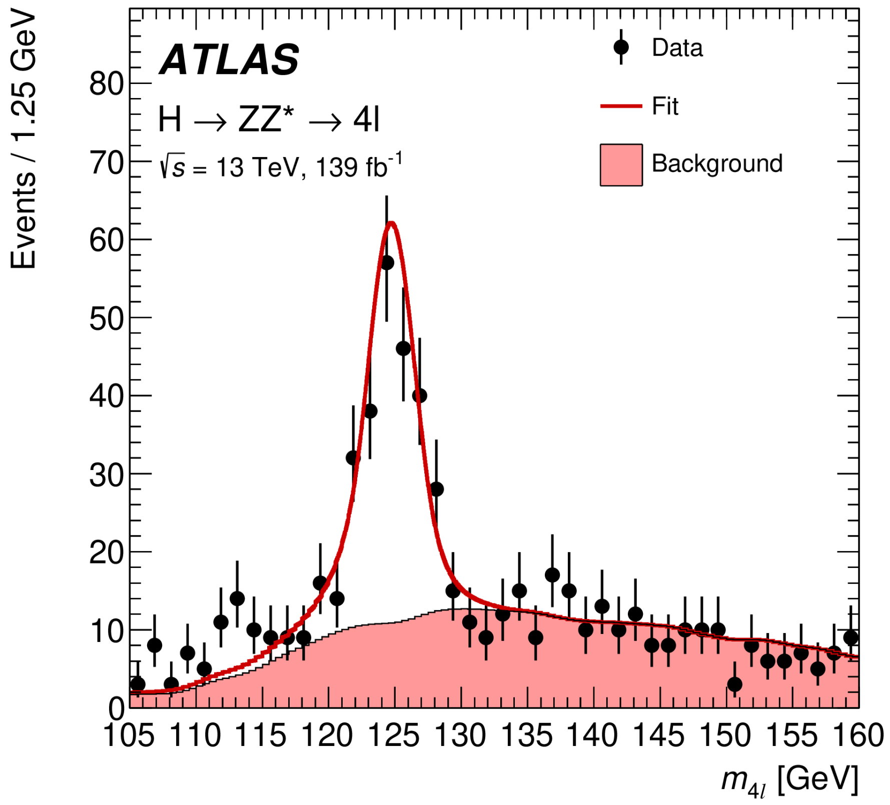

Latest result from 2023: Phys. Lett. B **843** (2023) 137880 using full Run 2 (139 fb^{-1})

Unbinned maximum likelihood fit

Signal = Breit Wigner ⊗ $m_{4\ell}$ response

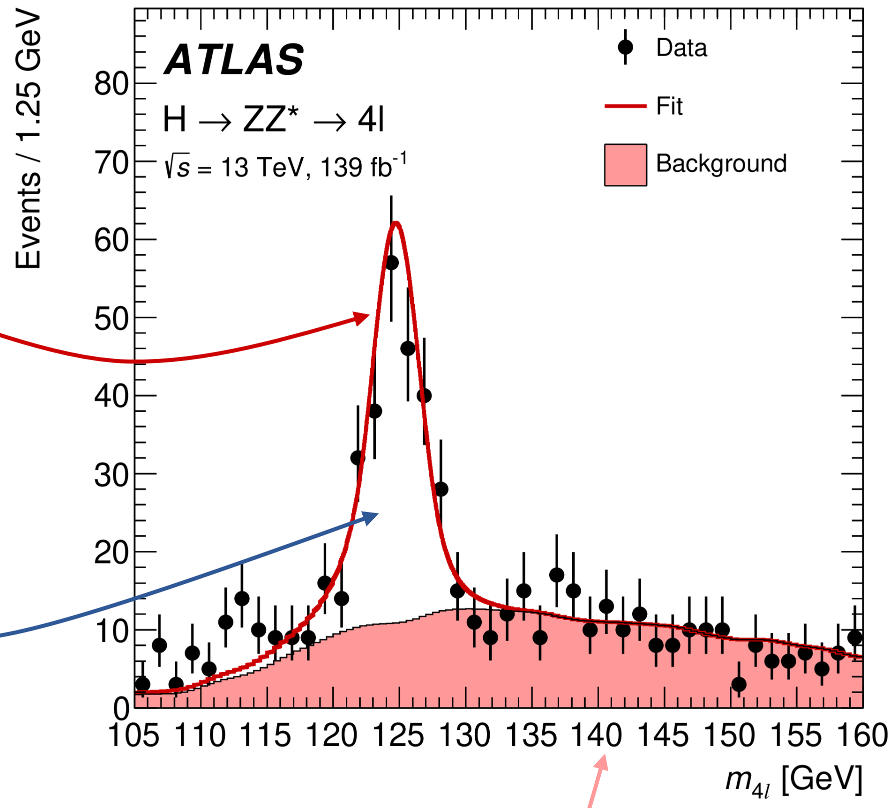

Background = non-resonant ZZ^*, VVV, tXX (MC-based) + mis-identified leptons (data-driven)

Mass measurement in $H \rightarrow ZZ^* \rightarrow 4\ell$

Latest result from 2023: [Phys. Lett. B **843** (2023) 137880] using full Run 2 (139 fb^{-1})

Unbinned maximum likelihood fit

Signal = Breit Wigner ⊗ $m_{4\ell}$ response

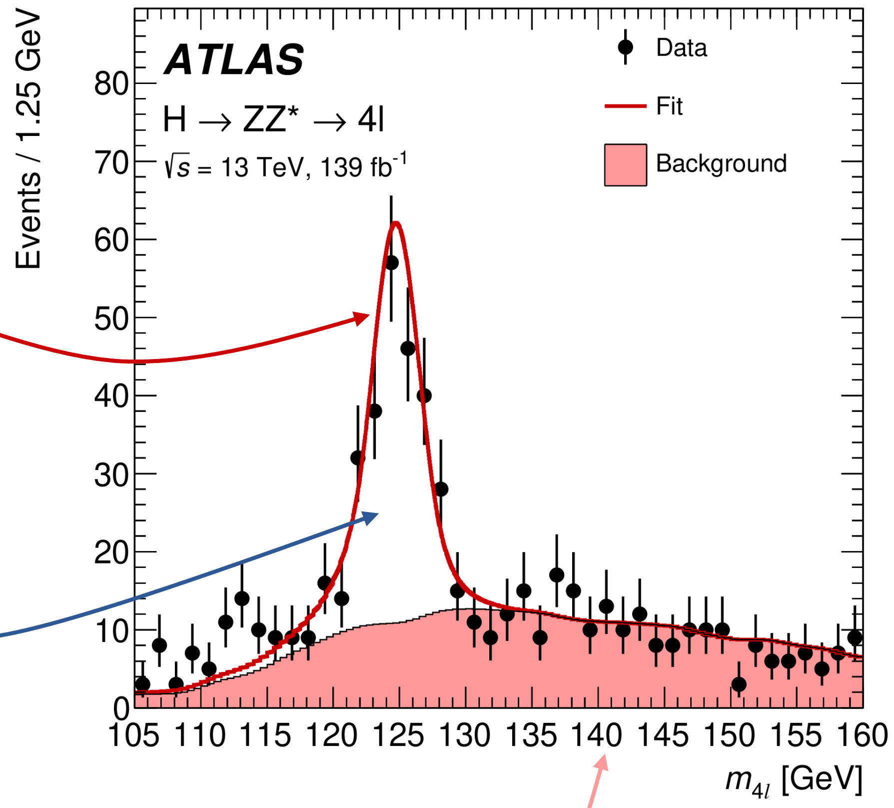

Background = non-resonant ZZ^*, VVV, tXX (MC-based) + mis-identified leptons (data-driven)

Improvements with respect to [partial Run 2 result]:

- Deep Neural Network (NN) to separate signal from background → used to parameterize signal and background models.
- Quantile Regression NN to estimate per-event resolution → used to parameterize width of $m_{4\ell}$ response in signal model.
- Improved muon momentum scale → **factor 4 reduction** in associated uncertainty.

Mass measurement in $H \to \gamma\gamma$ and $H \to ZZ^*$

Latest combination from 2023: Phys. Rev. Lett. **131** (2023) 251802 using full Run 2 (140 fb^{-1})

Combine channels:

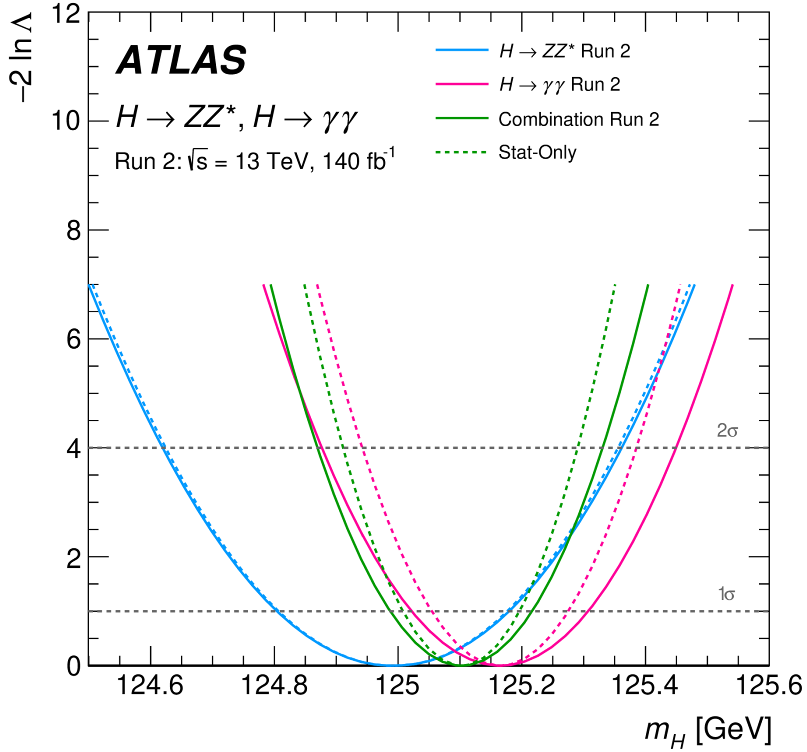

Stats and systematics ~equal for $H \to \gamma\gamma$

Stats dominate for $H \to ZZ^*$

Mass measurement in $H \to \gamma\gamma$ and $H \to ZZ^*$

Latest combination from 2023: Phys. Rev. Lett. **131** (2023) 251802 using full Run 2 (140 fb^{-1})

Combine channels:

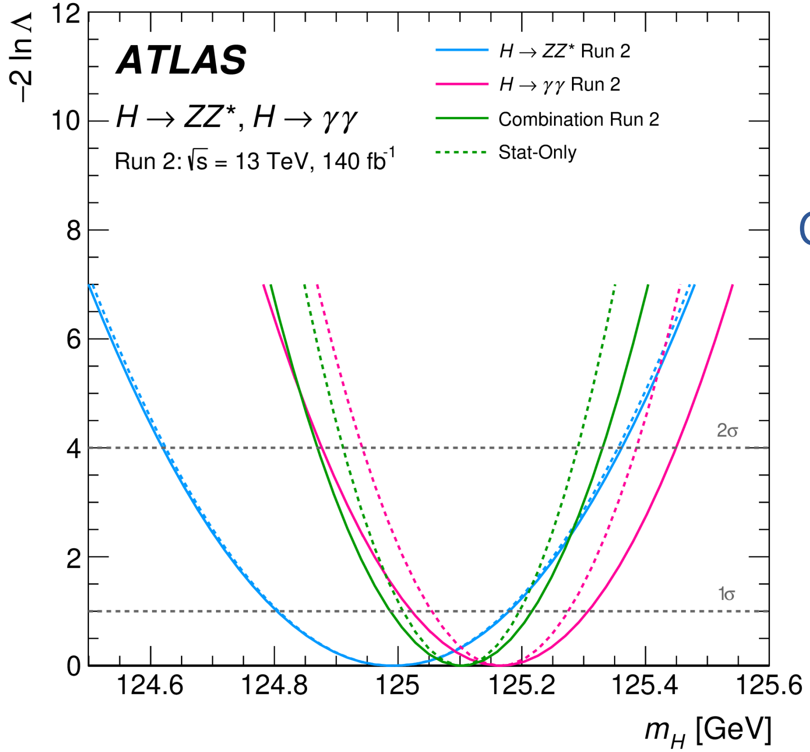

Combine with Run 1

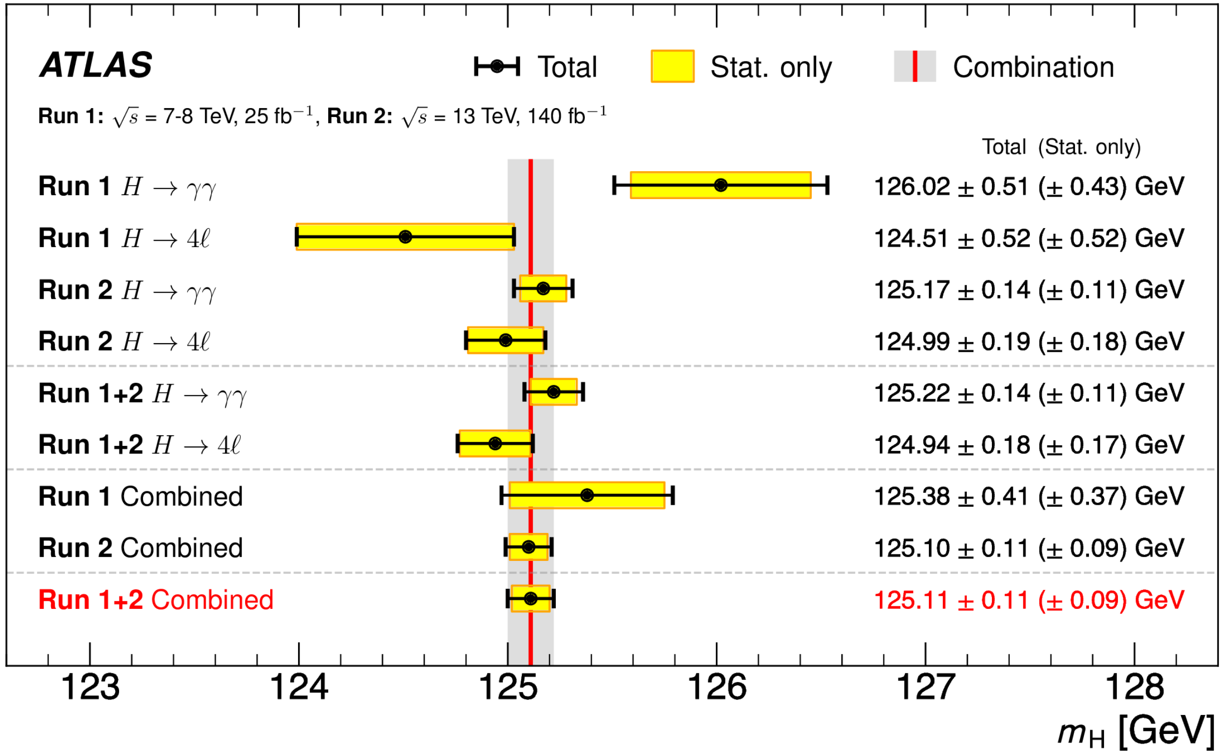

Stats and systematics ~equal for $H \to \gamma\gamma$

Stats dominate for $H \to ZZ^*$

0.09% precision achieved!

Width measurement

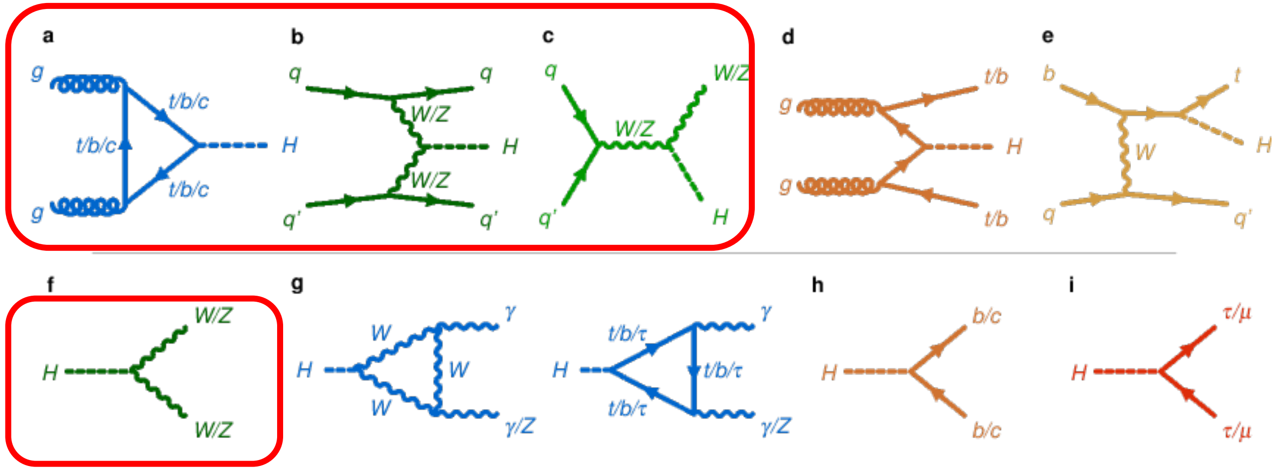

Introduction

- Theoretical Higgs width: $\Gamma_H = 4.1$ MeV, calculated from **all possible Higgs decays** → sensitive to any BSM particle that would interact with the Higgs.
- Not enough resolution to measure Γ_H directly at the LHC → **indirect measurement** in $H \to VV$ $(V = W, Z)$:

$$\mu_{\text{on-shell}} = \kappa^2_{\text{prod}} \times \kappa^2_{\text{decay}} \times \frac{1}{\kappa_H}$$

$$\mu_{\text{off-shell}} = \kappa^2_{\text{prod}} \times \kappa^2_{\text{decay}}$$

$\kappa_H = \Gamma_H / \Gamma_H^{SM}$

$\kappa_i = g_i / g_i^{SM}$

$$\Rightarrow \frac{\mu_{\text{off-shell}}}{\mu_{\text{on-shell}}} = \kappa_H$$

(assuming $\kappa_{i,\text{on-shell}} = \kappa_{i,\text{off-shell}}$)

- Off-shell $H^* \to VV$ slightly enhanced because the vector bosons become on-shell.
- **Destructive interference** in off-shell regime:
  ggH ↔ non-resonant VV and VBFH ↔ non-resonant $VVjj$
  ⇒ deficit in events compared to background-only.

Width measurement in $H \to WW \to \ell\nu\ell\nu$

Full Run 2 analysis (140 fb^{-1}) from April 2025: [arxiv:2504.07710] (submitted to Phys Lett. B.)

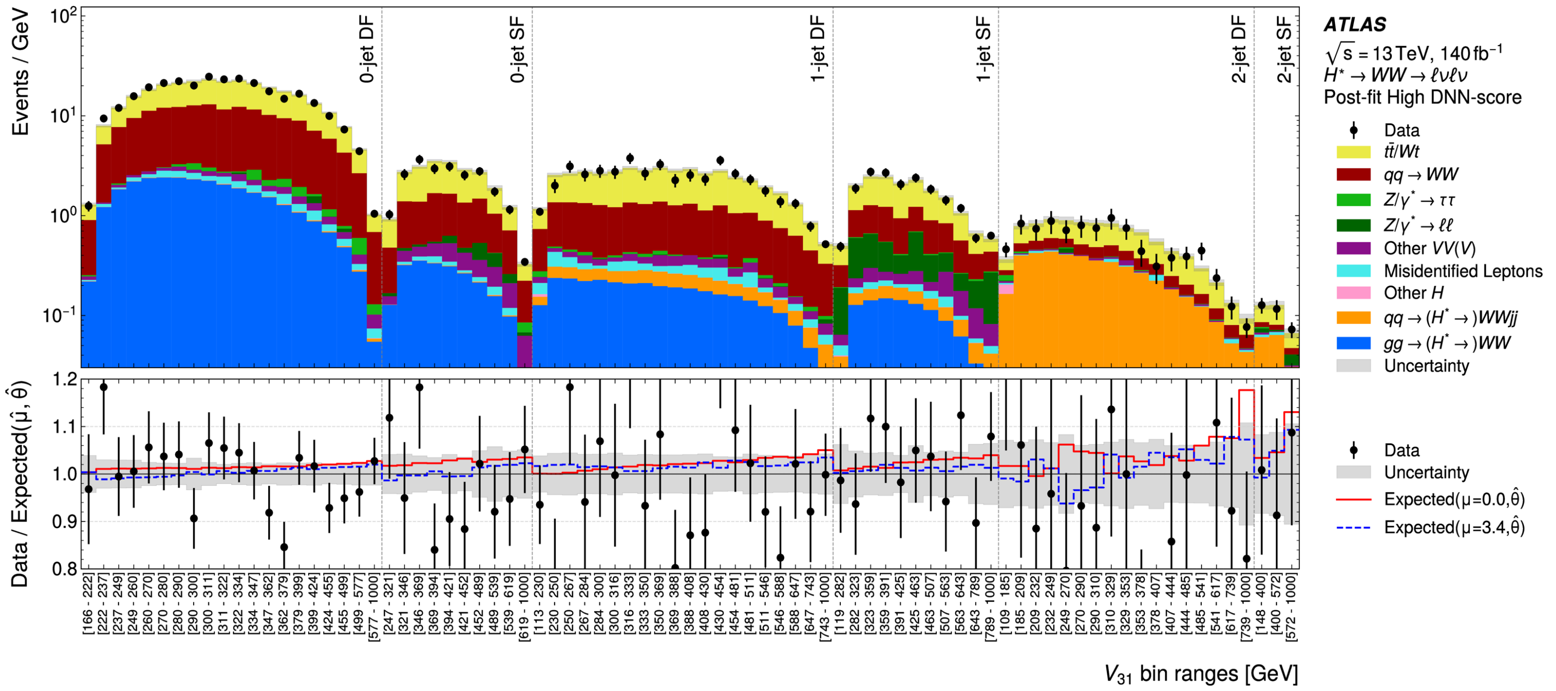

Width measurement in $H \to WW \to \ell\nu\ell\nu$

Full Run 2 analysis (140 fb[-1]) from April 2025: [arxiv:2504.07710](https://arxiv.org/abs/2504.07710) (submitted to Phys Lett. B.)

- Different Flavor (DF) and Same Flavor (SF) lepton selections
- 0, 1, and ≥ 2 jet selections

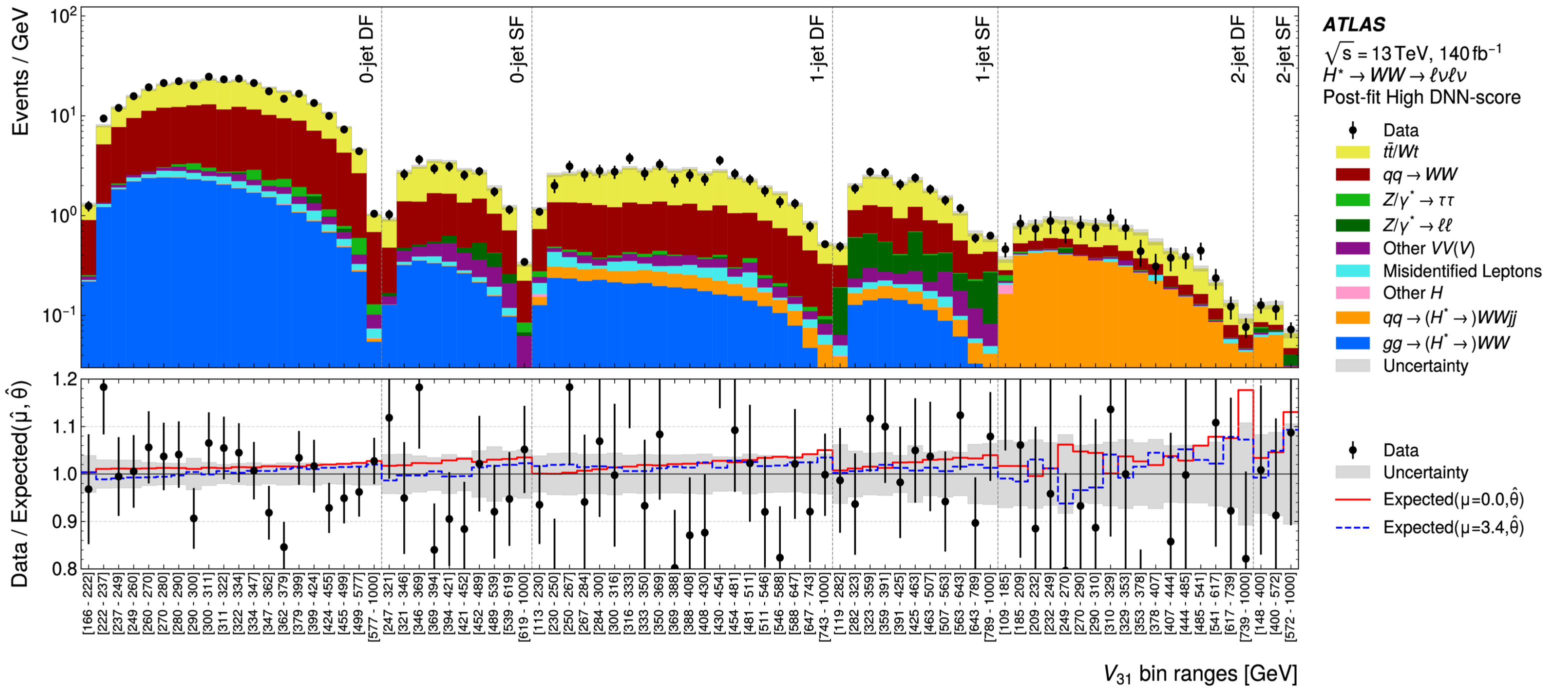

Width measurement in $H \rightarrow WW \rightarrow \ell\nu\ell\nu$

Full Run 2 analysis (140 fb^{-1}) from April 2025: arxiv:2504.07710 (submitted to Phys Lett. B.)

- Different Flavor (DF) and Same Flavor (SF) lepton selections
- 0, 1, and ≥ 2 jet selections

DNN to separate signal (with and without interference) from background → used to define regions in the fit

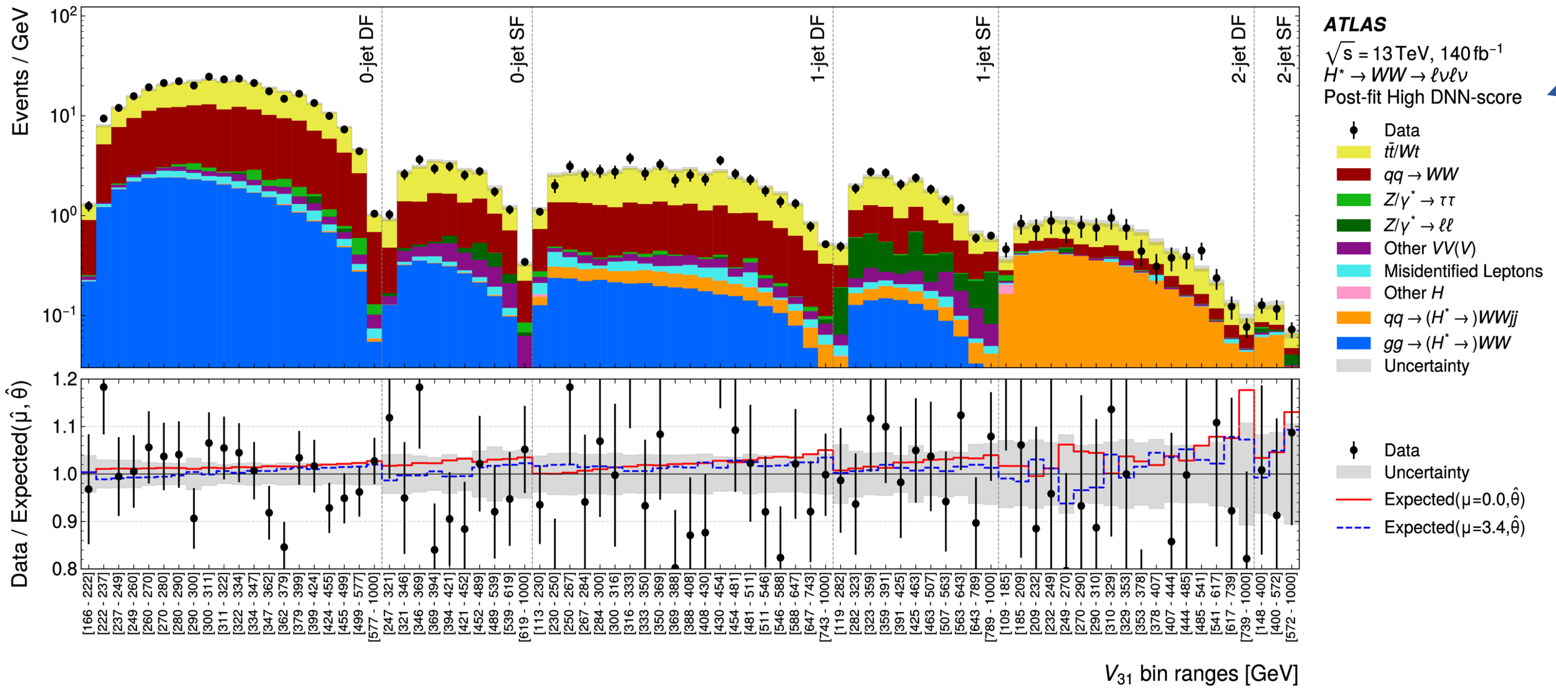

Width measurement in $H \to WW \to \ell\nu\ell\nu$

Full Run 2 analysis (140 fb^{-1}) from April 2025: arxiv:2504.07710 (submitted to Phys Lett. B.)

- Different Flavor (DF) and Same Flavor (SF) lepton selections
- 0, 1, and ≥ 2 jet selections

DNN to separate signal (with and without interference) from background → used to define regions in the fit

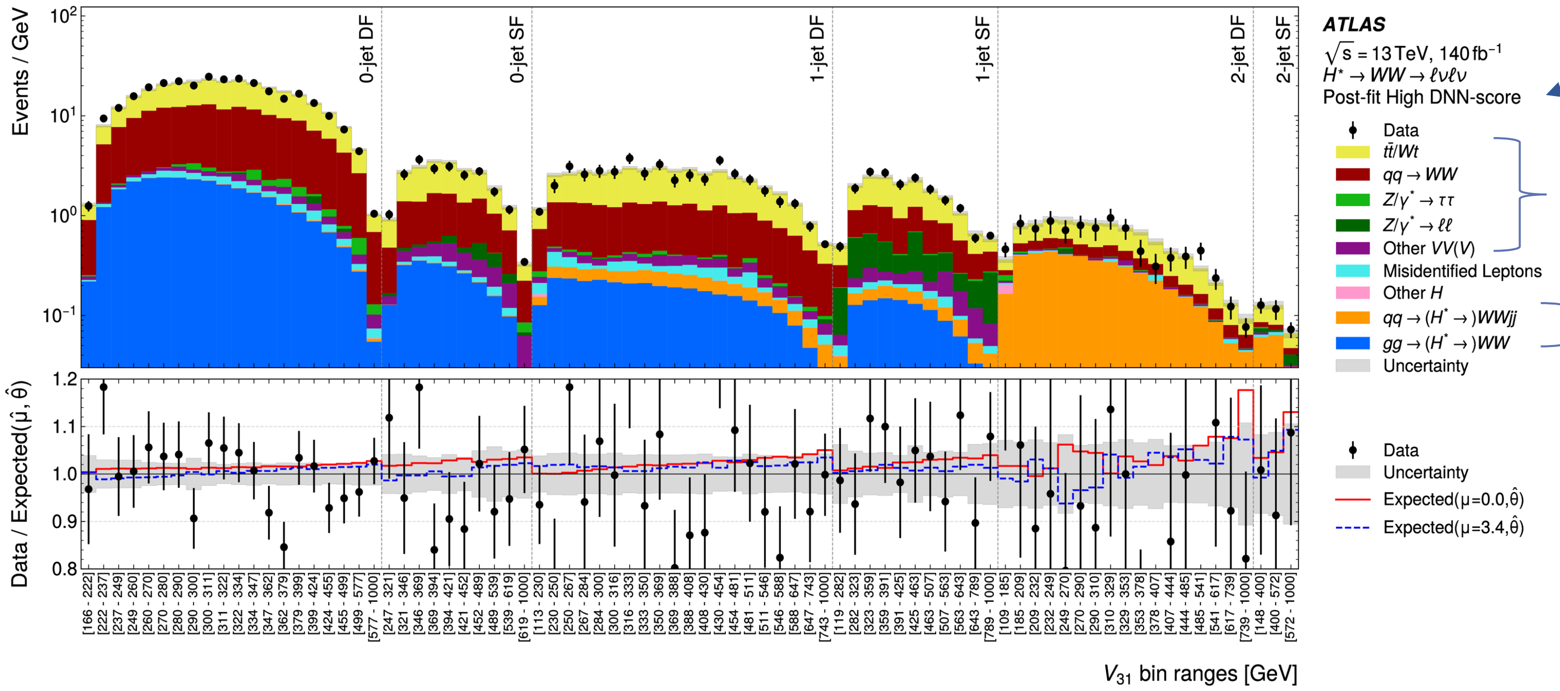

MC-based backgrounds (some normalized in control regions)

Mis-identified leptons background data-driven

Off-shell signal (ggH and VBF)

Width measurement in $H \to WW \to \ell\nu\ell\nu$

Full Run 2 analysis (140 fb[-1]) from April 2025: arxiv:2504.07710 (submitted to Phys Lett. B.)

- Different Flavor (DF) and Same Flavor (SF) lepton selections
- 0, 1, and ≥ 2 jet selections

DNN to separate signal (with and without interference) from background → used to define regions in the fit

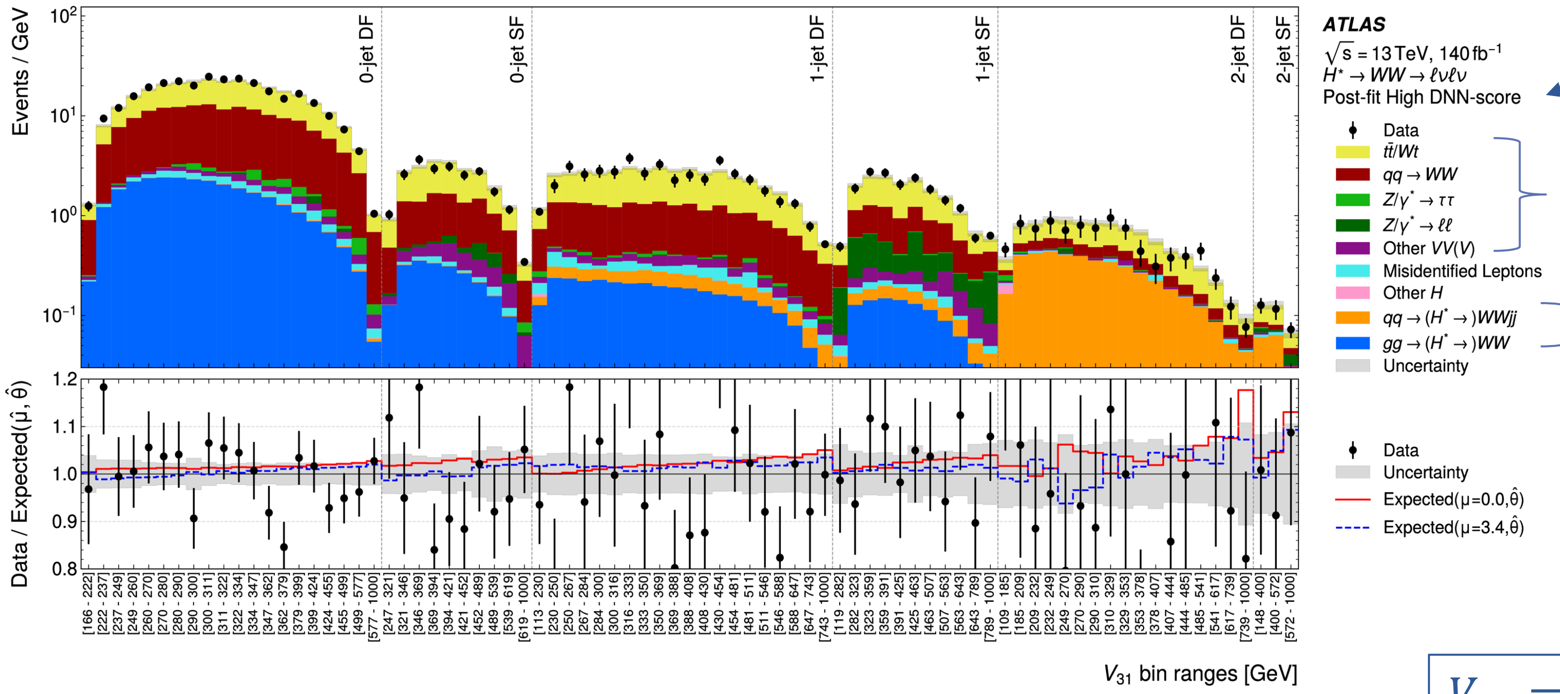

MC-based backgrounds (some normalized in control regions)

Mis-identified leptons background data-driven

Off-shell signal (ggH and VBF)

$V_{31} = 0.3 \times m_{\ell\ell} + 1 \times m_T \Rightarrow$ proxy for m_{WW}

Likelihood scan for $\mu_{\text{off-shell}}$:

(Confidence intervals from Neyman construction)

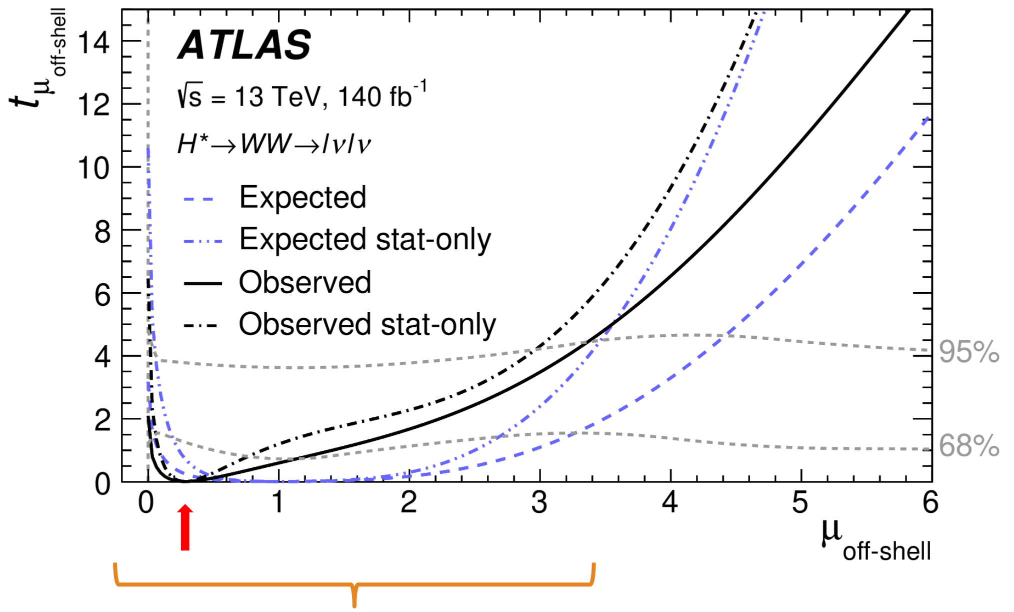

Best-fit: $\mu_{\text{off-shell}} = 0.3^{+0.9}_{-0.3}$ (expected $1.0^{+2.3}_{-1.0}$)

Upper limit: $\mu_{\text{off-shell}} \leq 3.4$ (expected 4.4)

Width measurement in $H \to WW \to \ell\nu\ell\nu$

Likelihood scan for $\mu_{\text{off-shell}}$:
(Confidence intervals from Neyman construction)

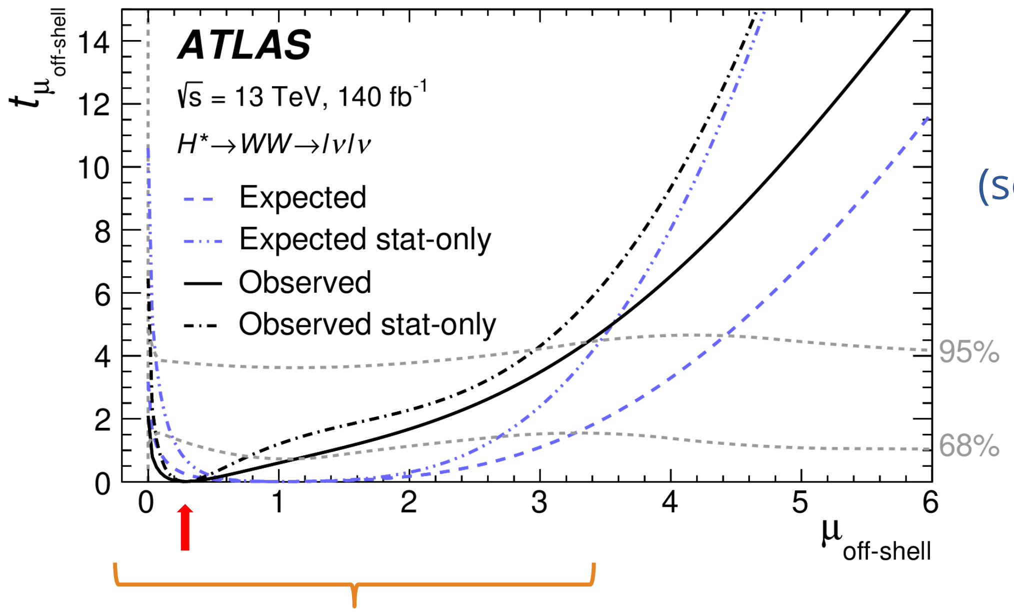

Take the ratio with $\mu_{\text{on-shell}}$
(see arxiv:2504.07686)

Likelihood scan for κ_H:

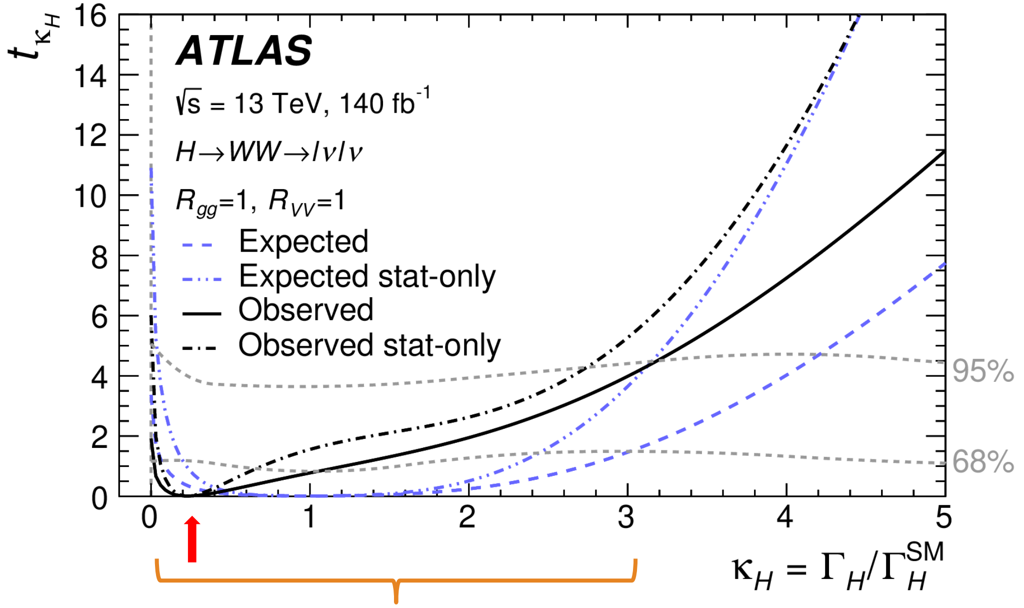

Best-fit: $\mu_{\text{off-shell}} = 0.3^{+0.9}_{-0.3}$ (expected $1.0^{+2.3}_{-1.0}$)

Upper limit: $\mu_{\text{off-shell}} \leq 3.4$ (expected 4.4)

Best-fit: $\Gamma_H = 0.9^{+3.4}_{-0.9}$ MeV (expected $4.1^{+8.3}_{-3.8}$ MeV)

Upper limit: $\Gamma_H \leq 13.1$ MeV (expected 17.3 MeV)

Compare with Run 1: $\Gamma_H \leq 17.2$ MeV (expected 21.3 MeV)

Width measurement in $H \to ZZ \to 4\ell$

Full Run 2 analysis (140 fb^{-1}) published in May 2025: *Rep. Prog. Phys.* **88** (2025) 057803

Improves upon previous result from 2023 using same dataset (Phys. Lett. B **846** (2023) 138223)

Unique statistical approach to deal with non-linear signal model:

$$
\begin{aligned}
-2\ln\lambda(\mu,\theta,\alpha) = &-2 \sum_{\text{regions } (I)} \ln\left[\text{Pois}\left(N_I|\nu_I(\mu,\theta,\alpha)\right)\right] \\
&-2 \sum_{\text{events } (i)} \ln\left[\frac{p(x_i|\mu,\theta,\alpha)}{p_{\text{ref}}(x_i)}\right] \\
&+ \sum_{\text{systematics } (m)} (\alpha_m - a_m)^2 .
\end{aligned}
$$

See talk by Andrea Sciandra on Wednesday

Width measurement in $H \to ZZ \to 4\ell$

Full Run 2 analysis (140 fb^{-1}) published in May 2025: *Rep. Prog. Phys.* **88** (2025) 057803

Improves upon previous result from 2023 using same dataset (Phys. Lett. B **846** (2023) 138223)

Unique statistical approach to deal with non-linear signal model:

Poisson term for total yield in each region

$$-2\ln\lambda(\mu,\theta,\alpha) = -2\sum_{\text{regions }(I)} \ln\left[\text{Pois}\left(N_I|\nu_I(\mu,\theta,\alpha)\right)\right] - 2\sum_{\text{events }(i)} \ln\left[\frac{p(x_i|\mu,\theta,\alpha)}{p_{\text{ref}}(x_i)}\right] + \sum_{\text{systematics }(m)} (\alpha_m - a_m)^2 .$$

Control Region | Signal Region

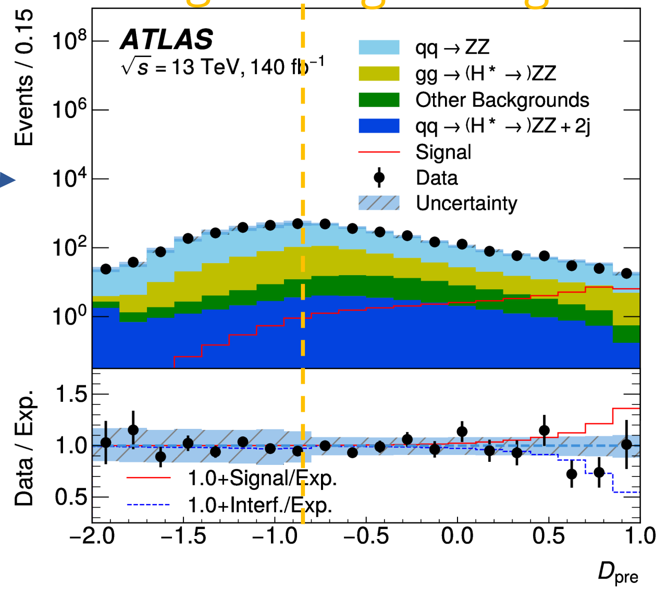

Initial multi-class NN to split events into signal and control regions.

See talk by Andrea Sciandra on Wednesday

Full Run 2 analysis (140 fb^{-1}) published in May 2025: *Rep. Prog. Phys.* **88** (2025) 057803

Improves upon previous result from 2023 using same dataset (Phys. Lett. B **846** (2023) 138223)

Unique statistical approach to deal with non-linear signal model:

$$-2\ln\lambda(\mu,\theta,\alpha) = -2\sum_{\text{regions }(I)} \ln\left[\text{Pois}\left(N_I|\nu_I(\mu,\theta,\alpha)\right)\right] - 2\sum_{\text{events }(i)} \ln\left[\frac{p(x_i|\mu,\theta,\alpha)}{p_{\text{ref}}(x_i)}\right] + \sum_{\text{systematics }(m)} (\alpha_m - a_m)^2 .$$

Poisson term for total yield in each region

Probability density ratios from Neural Simulation Based Inference (NSBI)

Control Region | Signal Region

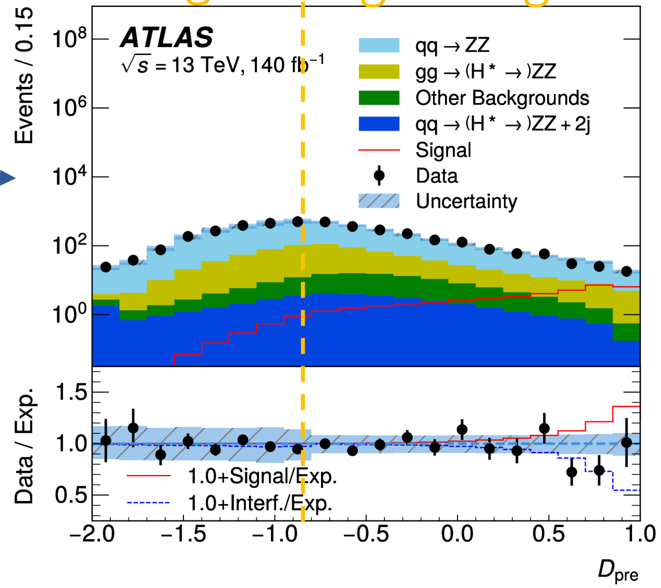

Initial multi-class NN to split events into signal and control regions.

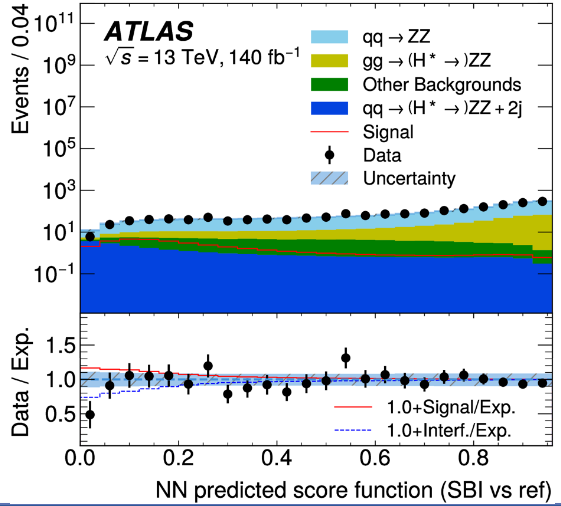

Estimate probability density ratio for each process (e.g. SBI = ggF signal+interference) as a function of 14 kinematic variables (x) using an ensemble of NNs.

See talk by Andrea Sciandra on Wednesday

Width measurement in $H \to ZZ \to 4\ell$

Likelihood scans for $\mu_{\text{off-shell}}$:

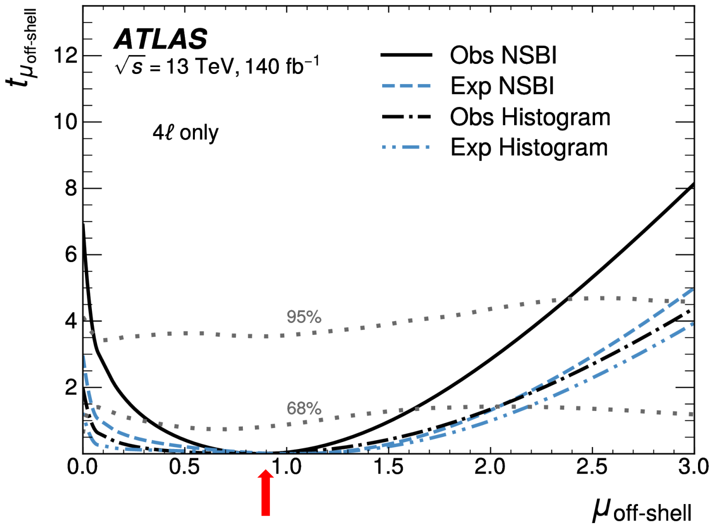

Best-fit: $\mu_{\text{off-shell}} = 0.87^{+0.75}_{-0.54}$

(expected $1.00^{+1.04}_{-0.95}$)

Significance: 2.5σ (expected 1.3σ)

Compare with previous ATLAS result using **same dataset**:

$\mu_{\text{off-shell}} = 0.79^{+1.21}_{-0.77}$, 0.8σ significance

Width measurement in $H \to ZZ \to 4\ell$

Likelihood scans for $\mu_{\text{off-shell}}$:

Combine with $H \to ZZ \to 2\ell 2\nu$
(*Phys. Lett. B* **846** (2023) 138223)

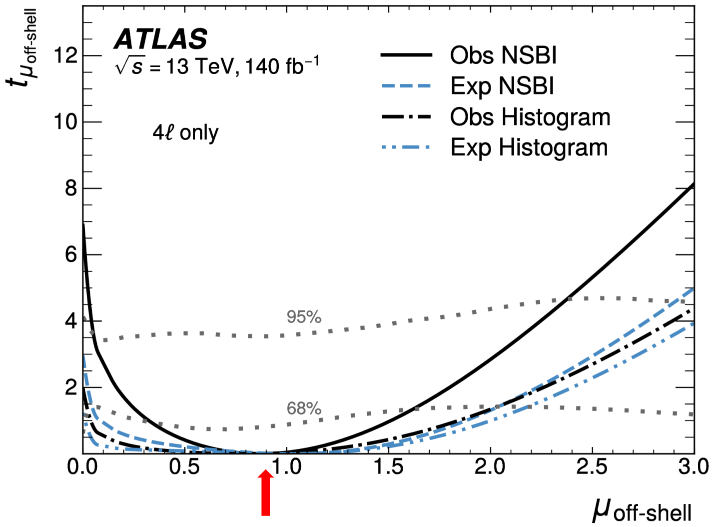

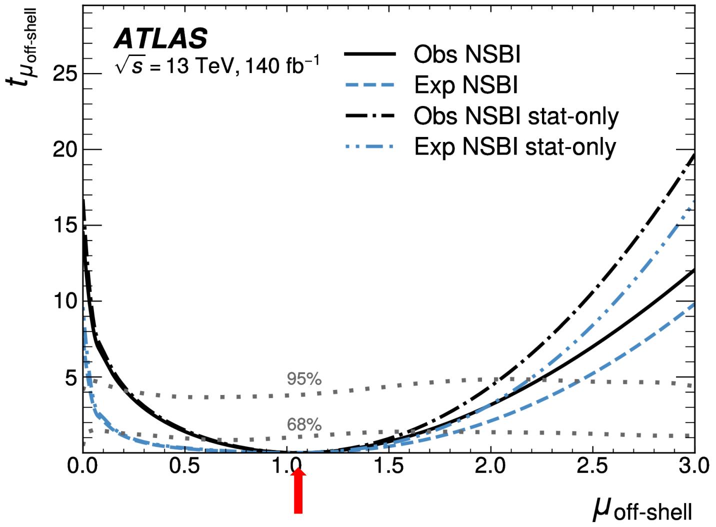

Best-fit: $\mu_{\text{off-shell}} = 0.87^{+0.75}_{-0.54}$
(expected $1.00^{+1.04}_{-0.95}$)
Significance: 2.5σ (expected 1.3σ)

Compare with previous ATLAS result using **same dataset**:
$\mu_{\text{off-shell}} = 0.79^{+1.21}_{-0.77}$, 0.8σ significance

Best-fit: $\mu_{\text{off-shell}} = 1.06^{+0.62}_{-0.45}$
(expected $1.00^{+0.83}_{-0.83}$)
Significance: 3.7σ (expected 2.4σ)

⇒ Clear evidence for off-shell Higgs production.

Width measurement in $H \to ZZ \to 4\ell$

Likelihood scans for $\mu_{\text{off-shell}}$:

Combine with $H \to ZZ \to 2\ell 2\nu$
(*Phys. Lett. B* **846** (2023) 138223)

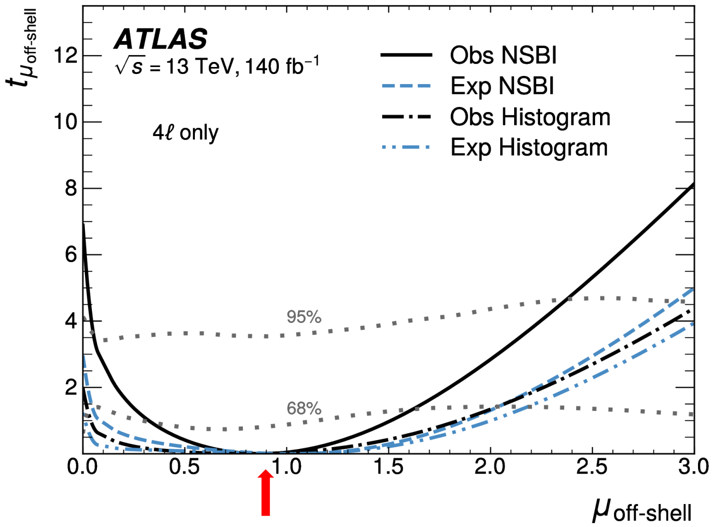

Best-fit: $\mu_{\text{off-shell}} = 0.87^{+0.75}_{-0.54}$
(expected $1.00^{+1.04}_{-0.95}$)
Significance: 2.5σ (expected 1.3σ)

Compare with previous ATLAS result using **same dataset**:
$\mu_{\text{off-shell}} = 0.79^{+1.21}_{-0.77}$, 0.8σ significance

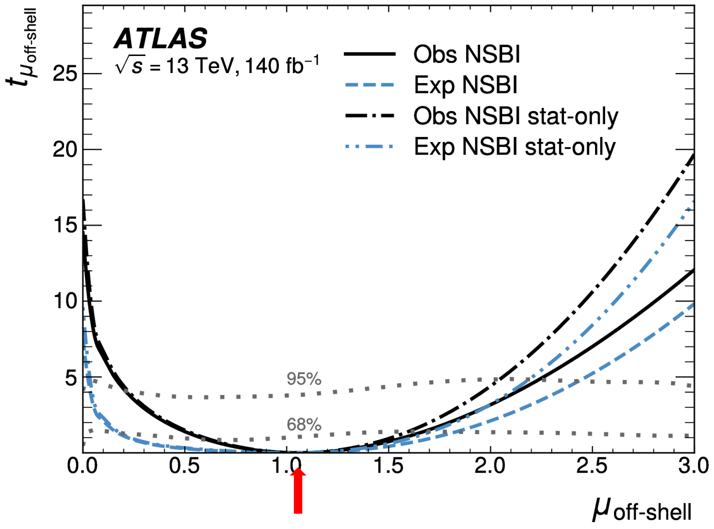

Best-fit: $\mu_{\text{off-shell}} = 1.06^{+0.62}_{-0.45}$
(expected $1.00^{+0.83}_{-0.83}$)
Significance: 3.7σ (expected 2.4σ)

⇒ Clear evidence for off-shell Higgs production.

Likelihood scan for κ_H:

Take the ratio with $\mu_{\text{on-shell}}$
(*Eur. Phys. J. C* **80** (2020) 957)

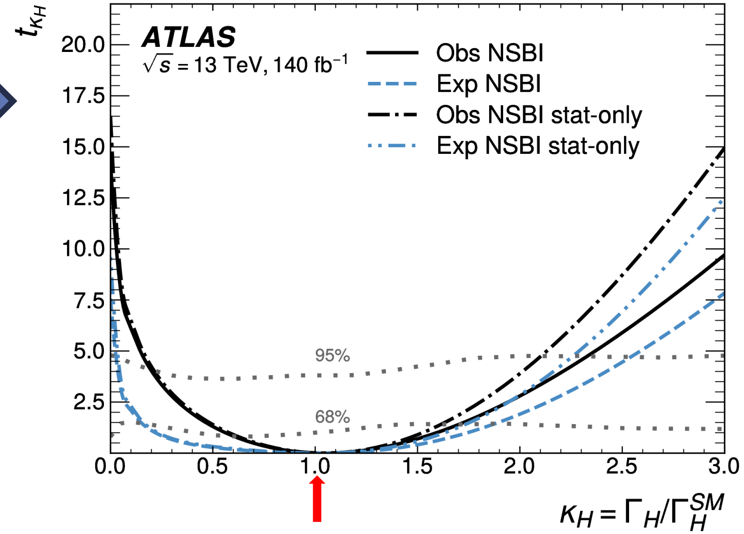

Best-fit: $\Gamma_H = 4.3^{+2.7}_{-1.9}$ MeV
(expected $4.1^{+3.5}_{-3.4}$)

Charge-Parity measurement

...

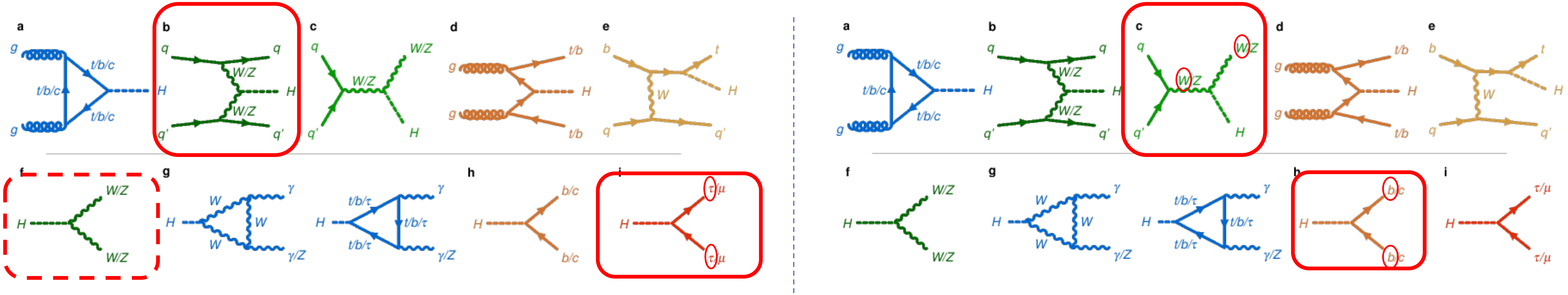

Introduction

- In SM, **Higgs is CP-even** → CP violation would be a sign of new physics → need to search for it in as many interaction vertices as possible. Focusing here on HVV vertex.
- **Effective Field Theory** (EFT):

$$\mathcal{L}_{EFT} = \mathcal{L}_{SM} + \sum_i \frac{c_i^{(d)}}{\Lambda^{(d-4)}} O_i^{(d)}$$

- Identify CP-odd dimension-6 terms:
  - HISZ basis: $\tilde{c}_{H\gamma\gamma}, \tilde{c}_{H\gamma Z}, \tilde{c}_{ZZ}, \tilde{c}_{WW}$ → can all be parameterized by a single parameter $\tilde{d}$, assuming $\tilde{c}_{H\gamma Z} = 0$.
  - Warsaw basis: $c_{H\widetilde{W}}, c_{H\tilde{B}}, c_{H\widetilde{W}B}$ → HVV CP analyses mostly sensitive to $c_{H\widetilde{W}}$.

  ⇒ Deviations from 0 indicate new physics.
- **Interference** between SM and CP-odd term causes CP violation effects.

CP measurement in VBF $H \rightarrow \tau\tau$

Brand new full Run 2 analysis (140 fb^{-1}) from June 2025: arxiv:2506.19395 (submitted to JHEP)

Sensitive variable: Optimal observable:

$$\mathcal{OO} = \frac{2\mathcal{R}(\mathcal{M}^*_{\text{SM}}\mathcal{M}_{\text{CP-odd}})}{{\mathcal{M}^*_{\text{SM}}}^2}$$

Matrix Elements calculated from kinematics of Higgs and VBF jets.

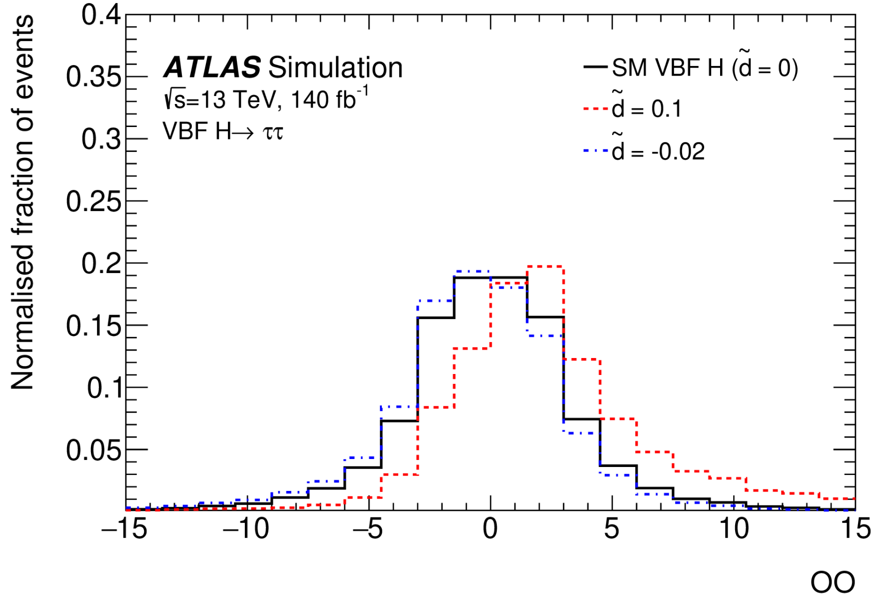

⇒ ~40% improvement in expected confidence interval for $\tilde{d}$ compared to using $\Delta\phi_{jj}^{sign}$.

CP measurement in VBF $H \rightarrow \tau\tau$

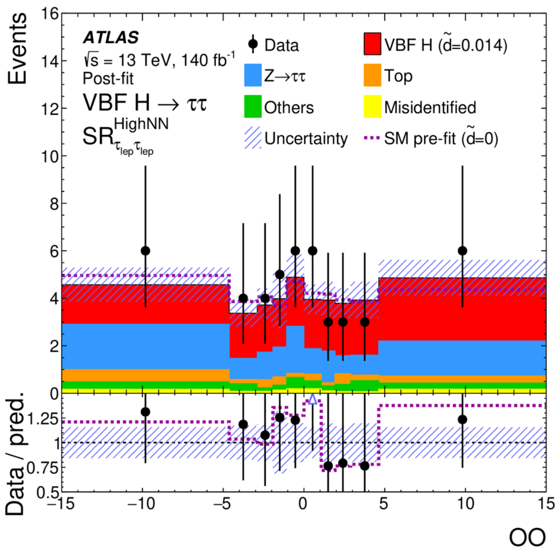

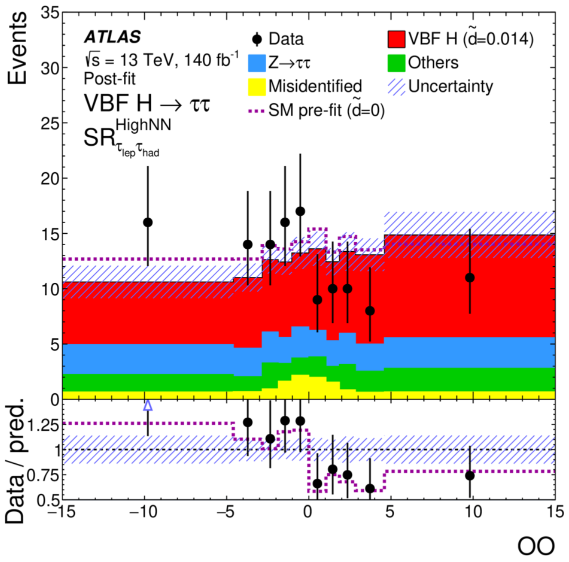

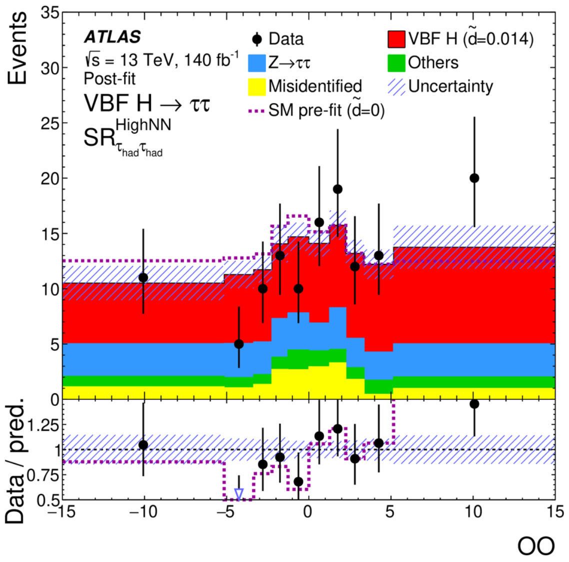

Optimal observable used as fitting variable

CP measurement in VBF $H \to \tau\tau$

Target VBF topology

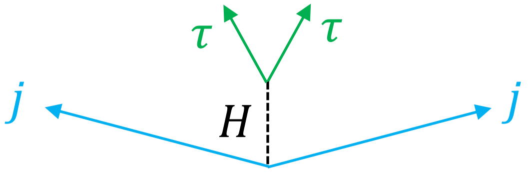

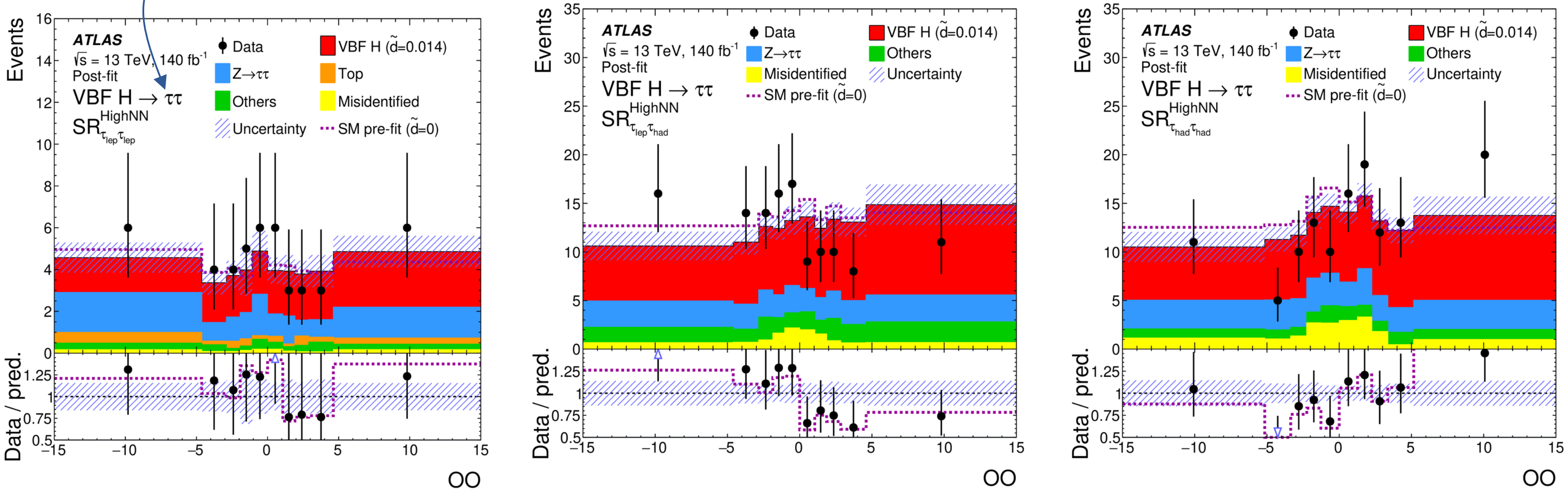

Optimal observable used as fitting variable

CP measurement in VBF $H \rightarrow \tau\tau$

Target VBF topology

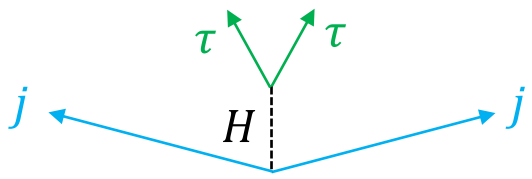

Channels: $\tau_{lep}\tau_{lep}$ ($e\mu$ only), $\tau_{lep}\tau_{had}$, $\tau_{had}\tau_{had}$

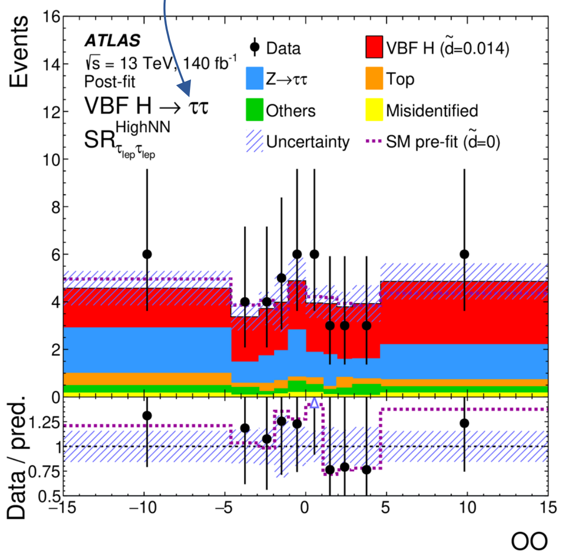

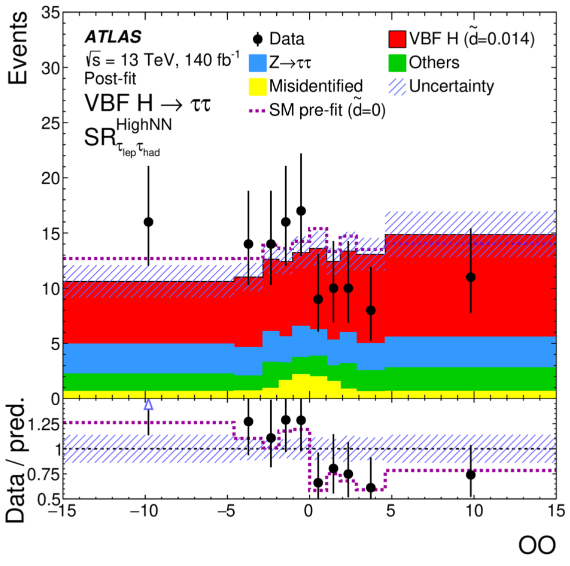

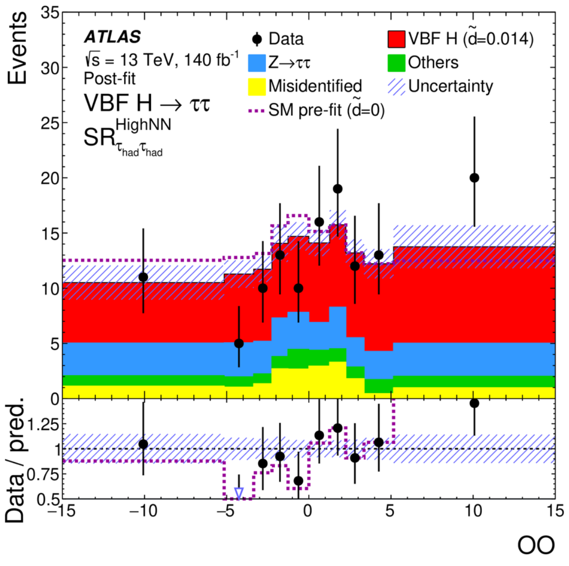

Optimal observable used as fitting variable

CP measurement in VBF $H \rightarrow \tau\tau$

Target VBF topology

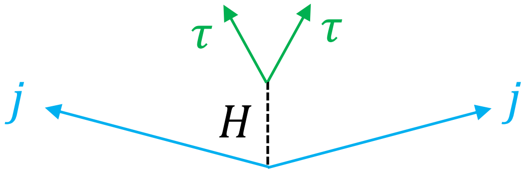

Channels: $\tau_{lep}\tau_{lep}$ ($e\mu$ only), $\tau_{lep}\tau_{had}$, $\tau_{had}\tau_{had}$

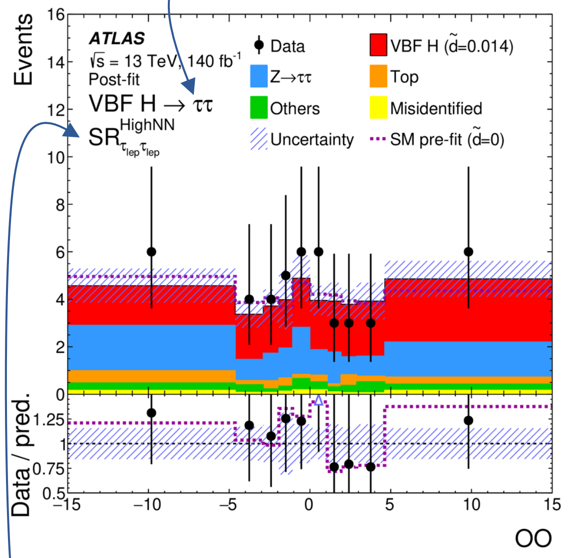

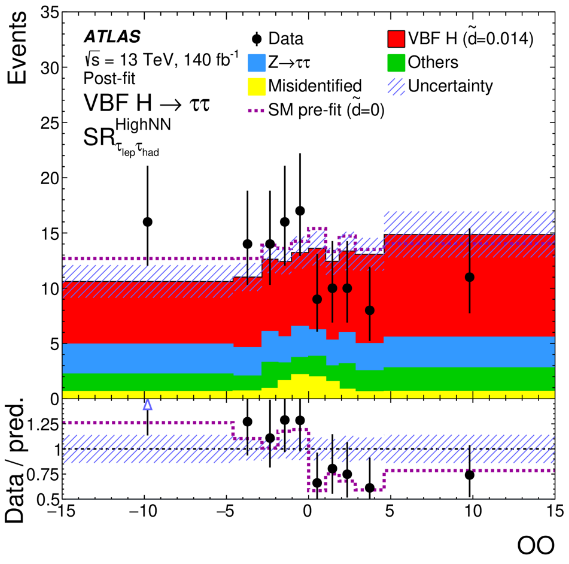

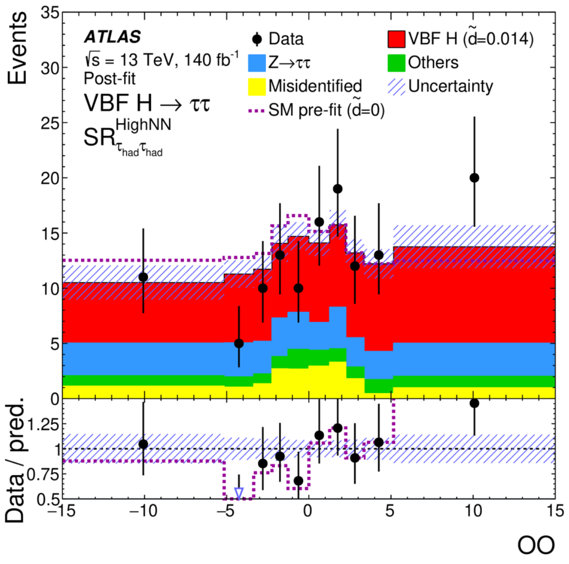

Optimal observable used as fitting variable

NN to separate signal (independent of CP) from background → used to define signal regions.

CP measurement in VBF $H \rightarrow \tau\tau$

Target VBF topology

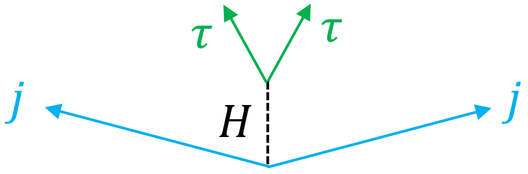

Channels: $\tau_{lep}\tau_{lep}$ ($e\mu$ only), $\tau_{lep}\tau_{had}$, $\tau_{had}\tau_{had}$

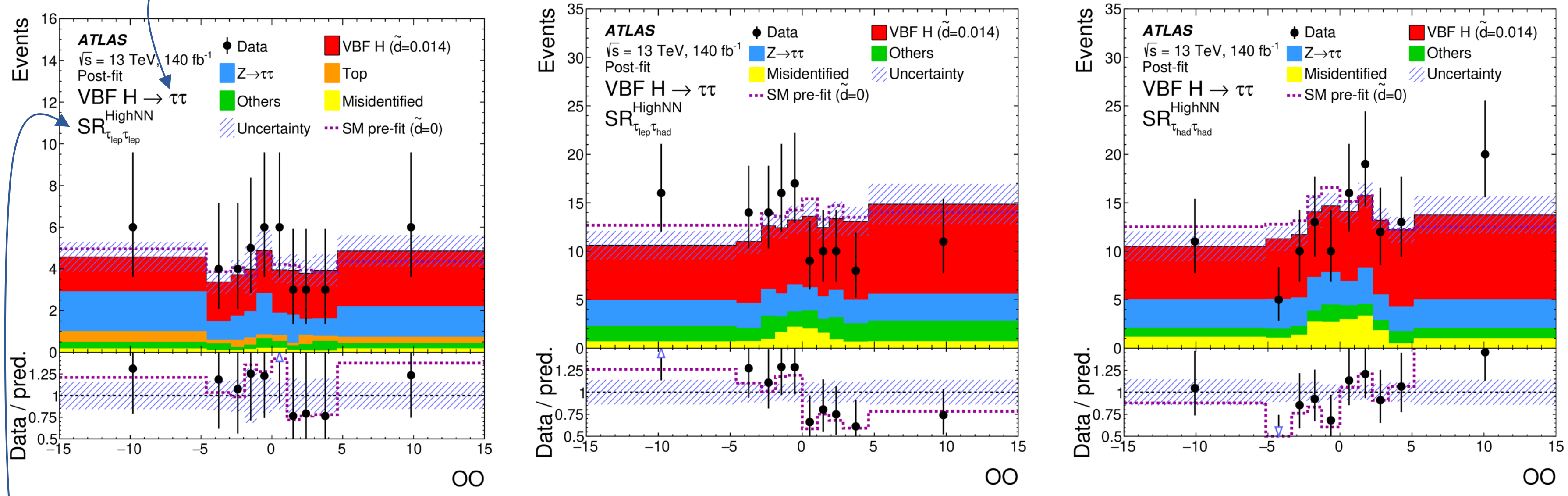

Optimal observable used as fitting variable

NN to separate signal (independent of CP) from background → used to define signal regions.

Background estimation:

- $Z\rightarrow\tau\tau$: object-level embedding: take $Z\rightarrow\ell\ell$ data and replace the ℓ's with τ's. Then use sample in same-flavor CR to constrain $Z\rightarrow\tau\tau$ normalization.
- Mis-identified: data-driven matrix method in $\tau_{lep}\tau_{lep}$ or fake factor method in $\tau_{lep}\tau_{had}$ and $\tau_{had}\tau_{had}$.
- Top: normalization from CR in $\tau_{lep}\tau_{lep}$.

CP measurement in VBF $H \to \tau\tau$

Likelihood scan for $\tilde{d}$:

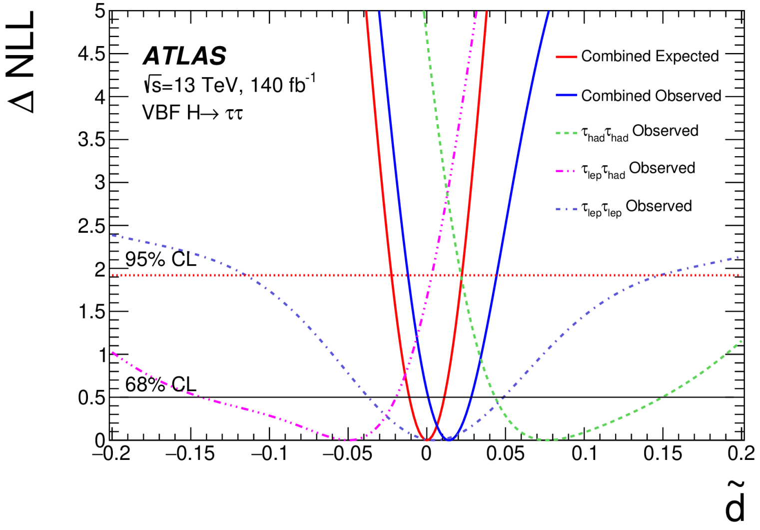

Likelihood scan for $c_{H\tilde{W}}$:

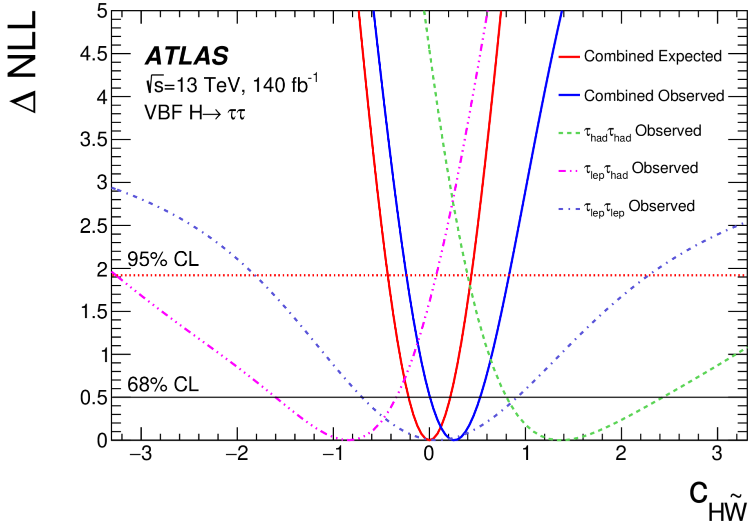

CP measurement in VBF $H \to \tau\tau$

Likelihood scan for $\tilde{d}$:

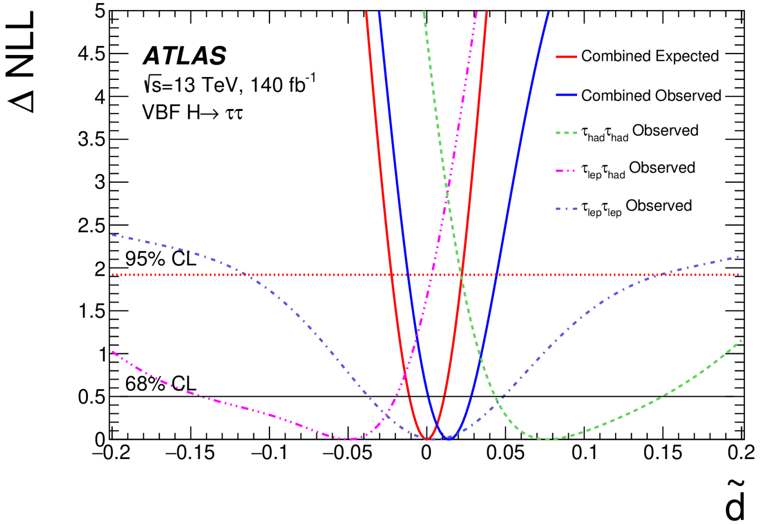

Likelihood scan for $c_{H\tilde{W}}$:

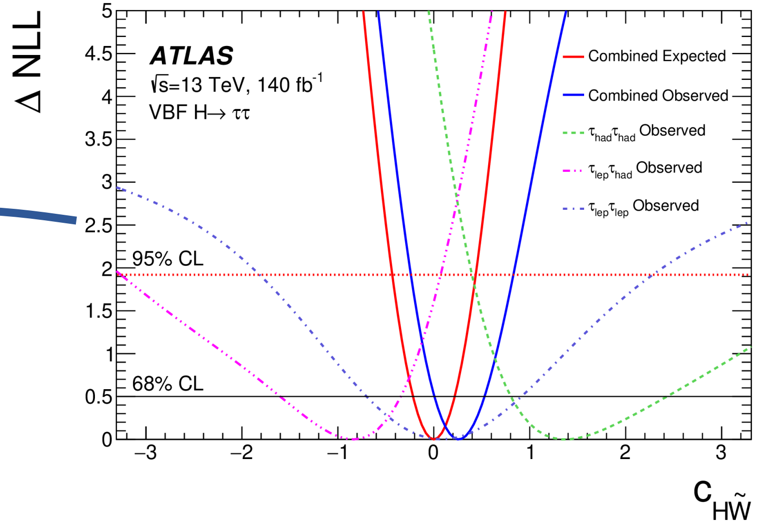

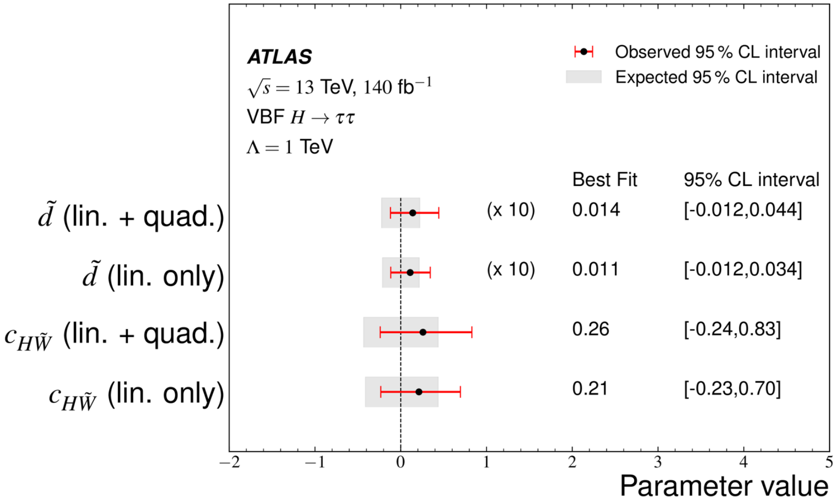

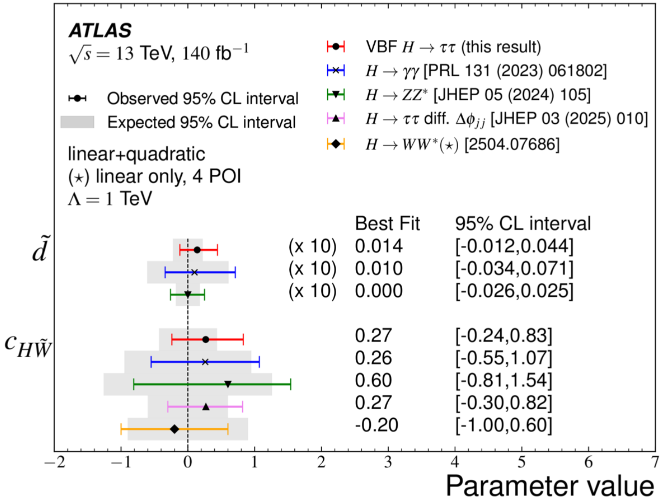

- Measurement dominated by statistical uncertainty.
- All CP-sensitive parameters compatible with 0.
- Among the most stringent limits of all channels.

CP measurement in $WH, H \to b\bar{b}$

Full Run 2 analysis (140 fb^{-1}) from May 2025: ATL-PHYS-PUB-2025-022

First CP study in VH production

Allows to probe HWW vertex specifically → only $c_{H\tilde{W}}$ is relevant

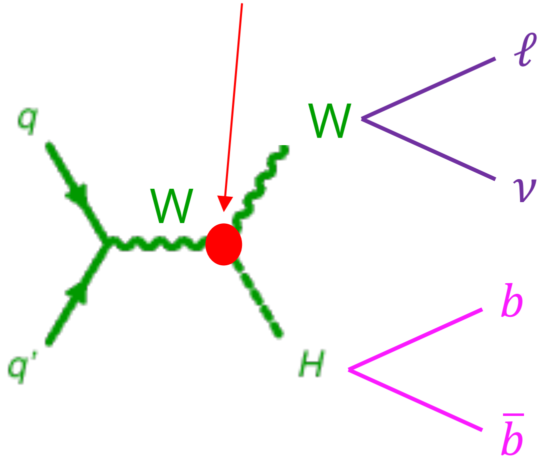

CP measurement in $WH, H \to b\bar{b}$

Full Run 2 analysis (140 fb[-1]) from May 2025: ATL-PHYS-PUB-2025-022

First CP study in VH production

Allows to probe HWW vertex specifically → only $c_{H\tilde{W}}$ is relevant

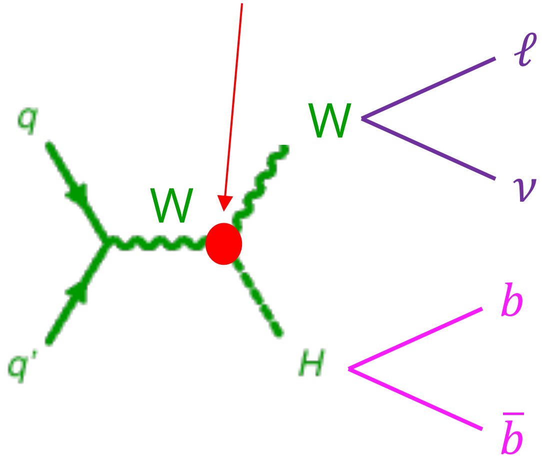

Sensitive variable:

$$Q_\ell \cos(\delta^+) = \frac{\boldsymbol{p}_\ell^{(W)} \cdot (\boldsymbol{p}_H \times \boldsymbol{p}_W)}{|\boldsymbol{p}_\ell^{(W)}| \cdot |(\boldsymbol{p}_H \times \boldsymbol{p}_W)|}$$

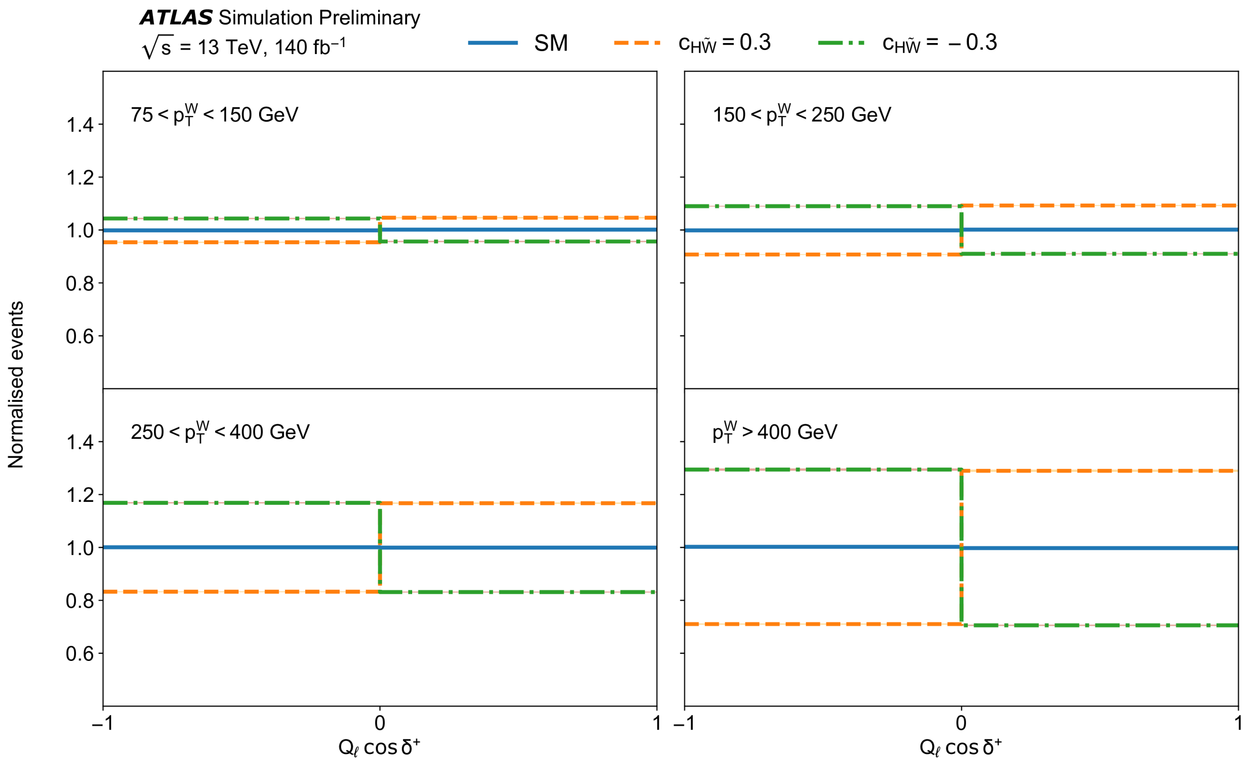

CP measurement in $WH, H \to b\bar{b}$

Each SR separated into $Q_\ell \cos(\delta^+) \leq 0$ and $Q_\ell \cos(\delta^+) > 0$

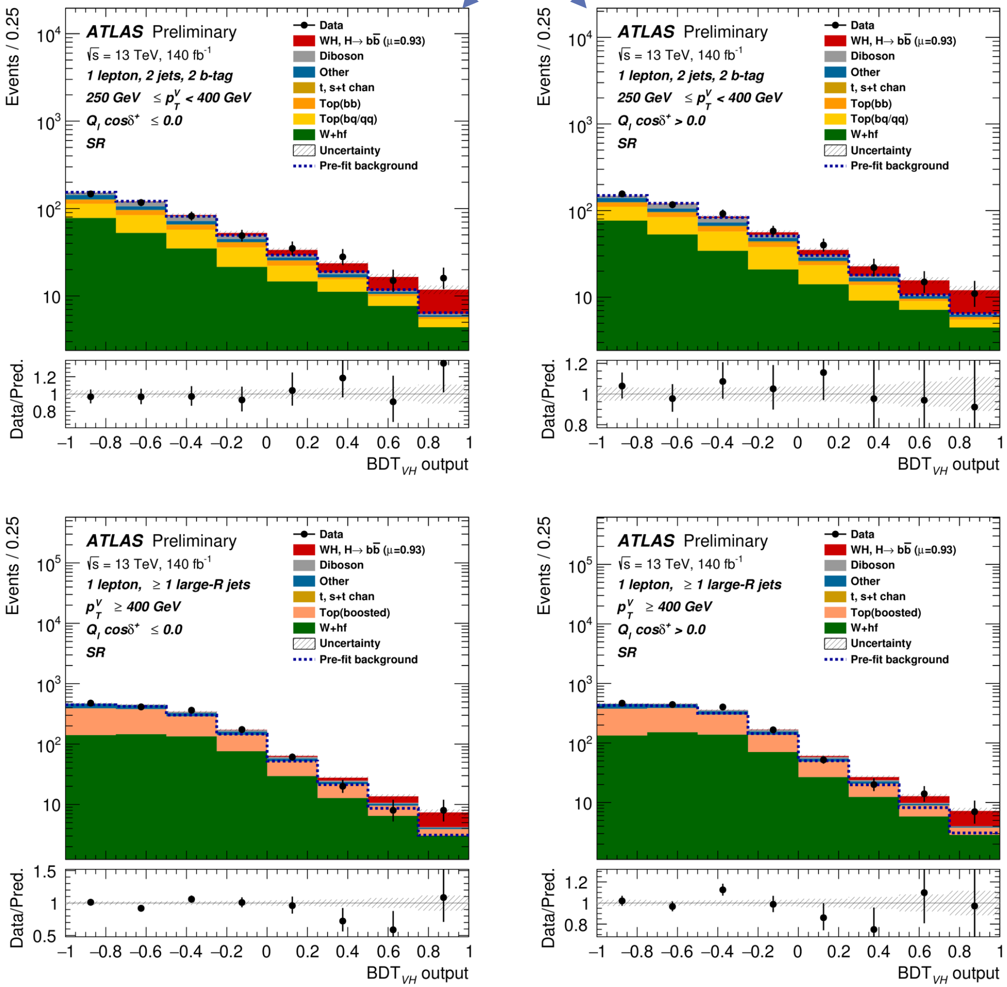

Each SR separated into $Q_\ell \cos(\delta^+) \le 0$ and $Q_\ell \cos(\delta^+) > 0$

Resolved ($p_T^W \le 400$ GeV) and boosted ($p_T^W \ge 400$ GeV) topologies. Resolved split into 3 p_T^W bins.

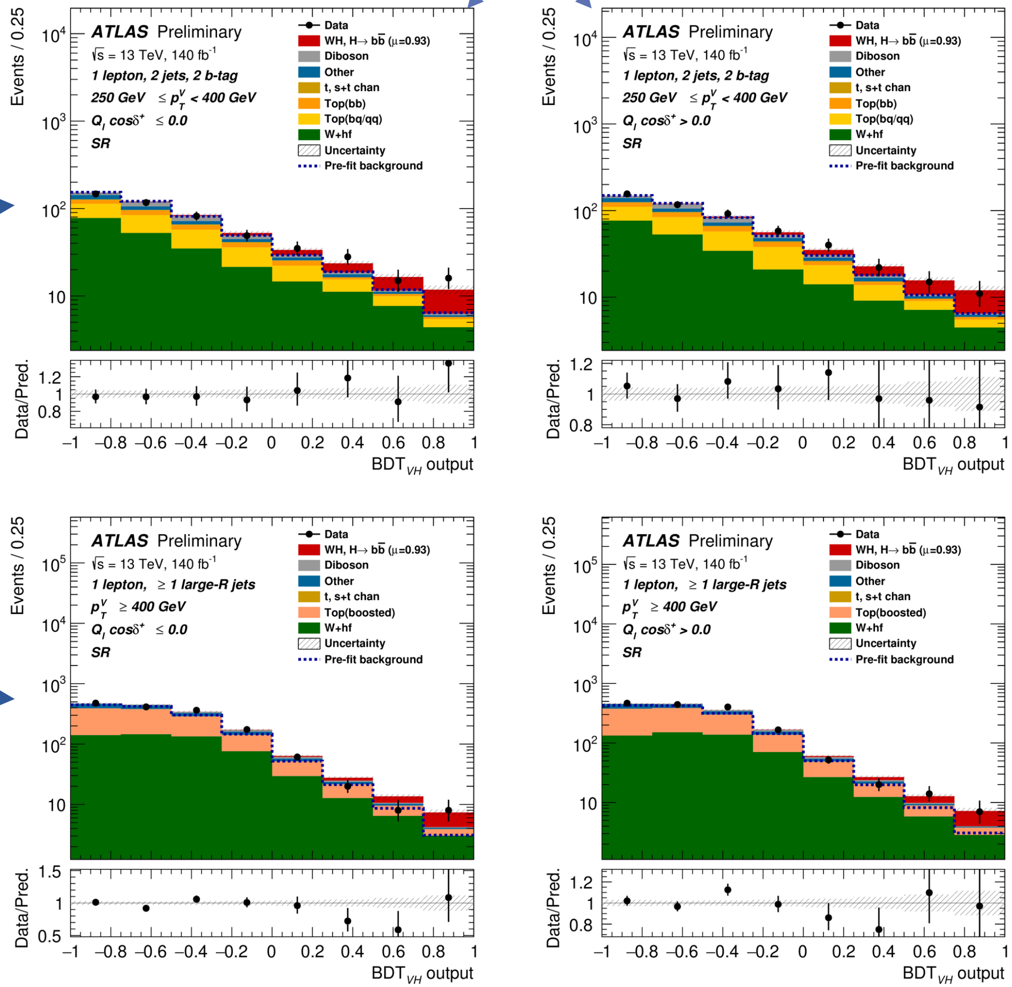

CP measurement in $WH, H \to b\bar{b}$

Each SR separated into $Q_\ell \cos(\delta^+) \leq 0$ and $Q_\ell \cos(\delta^+) > 0$

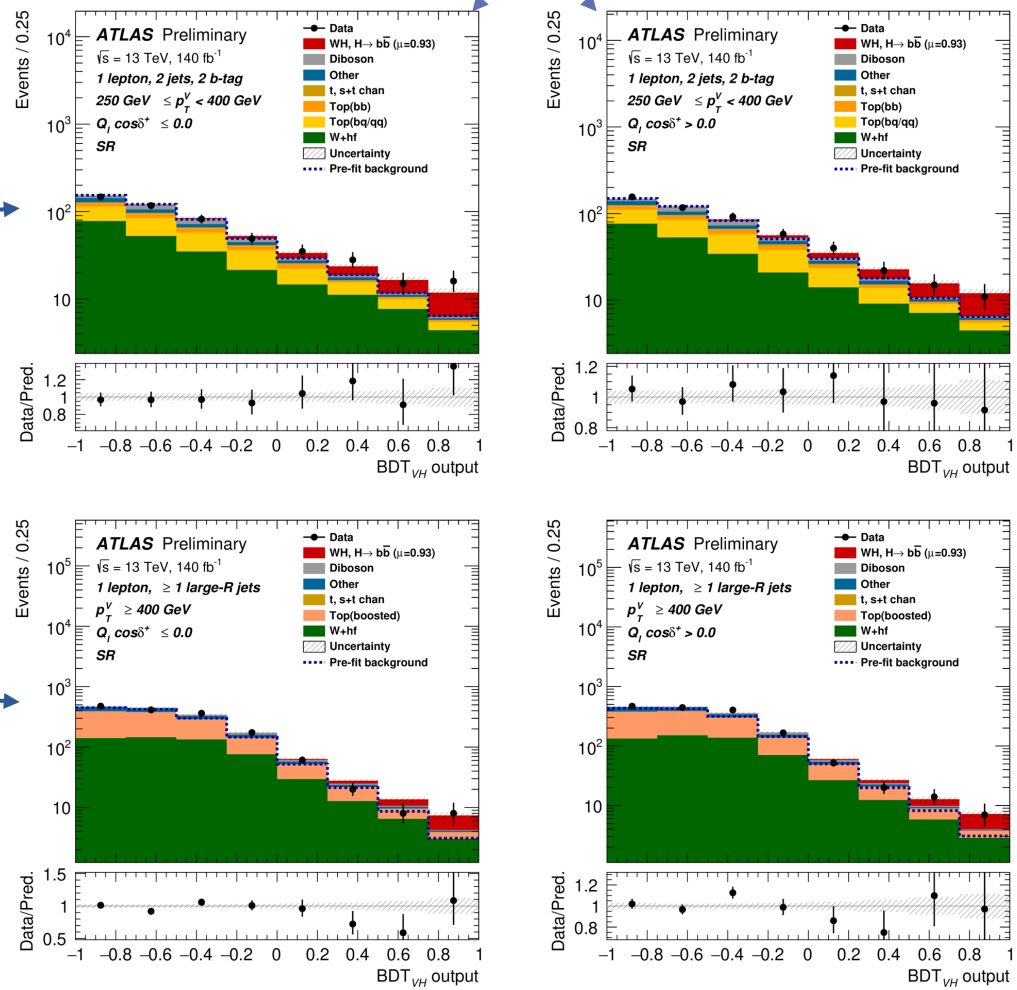

Resolved ($p_T^W \leq 400$ GeV) and boosted ($p_T^W \geq 400$ GeV) topologies. Resolved split into 3 p_T^W bins.

BDT score for separating VH from background used as fitting variable in signal regions

CP measurement in $WH, H \to b\bar{b}$

Each SR separated into $Q_\ell \cos(\delta^+) \le 0$ and $Q_\ell \cos(\delta^+) > 0$

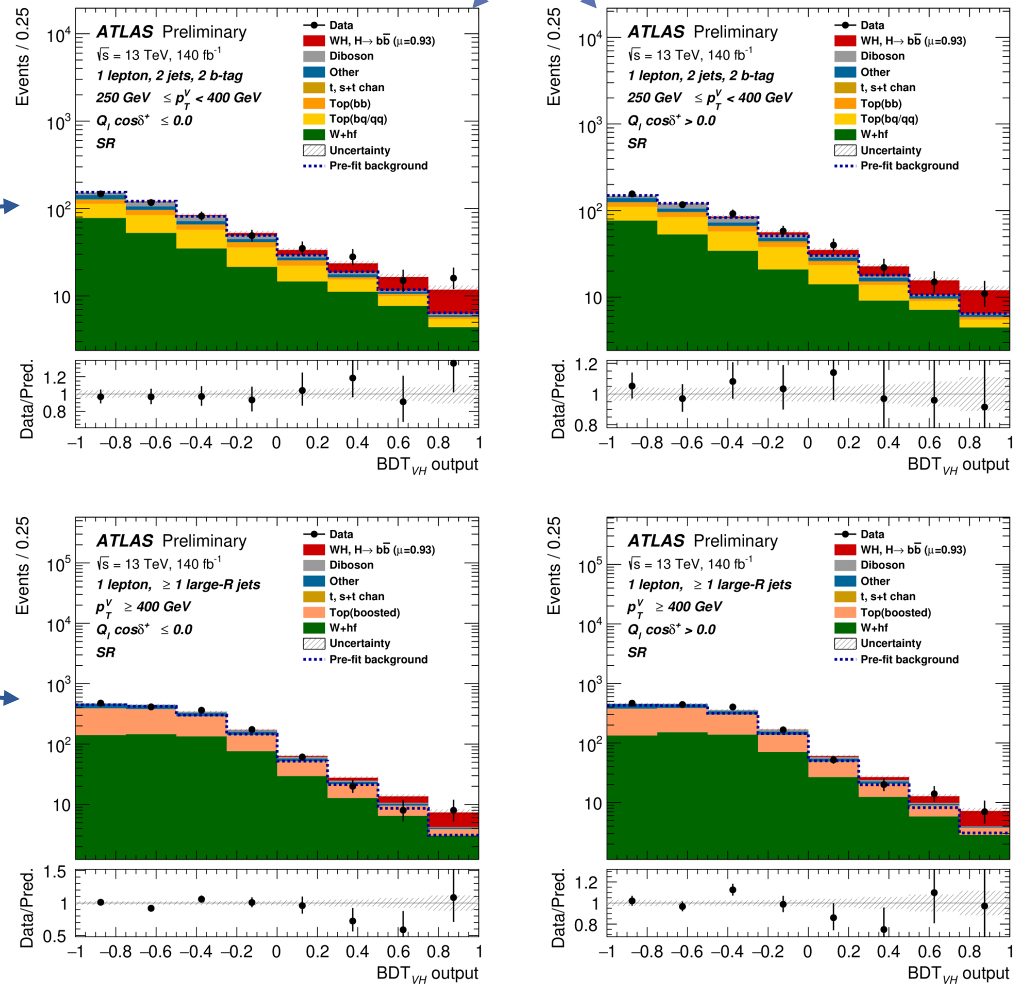

Resolved ($p_T^W \le 400$ GeV) and boosted ($p_T^W \ge 400$ GeV) topologies. Resolved split into 3 p_T^W bins.

BDT score for separating VH from background used as fitting variable in signal regions

Backgrounds:

- Normalization of W+jets constrained in control regions defined by ΔR_{bb}
- Normalization of Top backgrounds constrained in control regions defined by ΔR_{bb} and b/c-tagging.

CP measurement in $WH, H \to b\bar{b}$

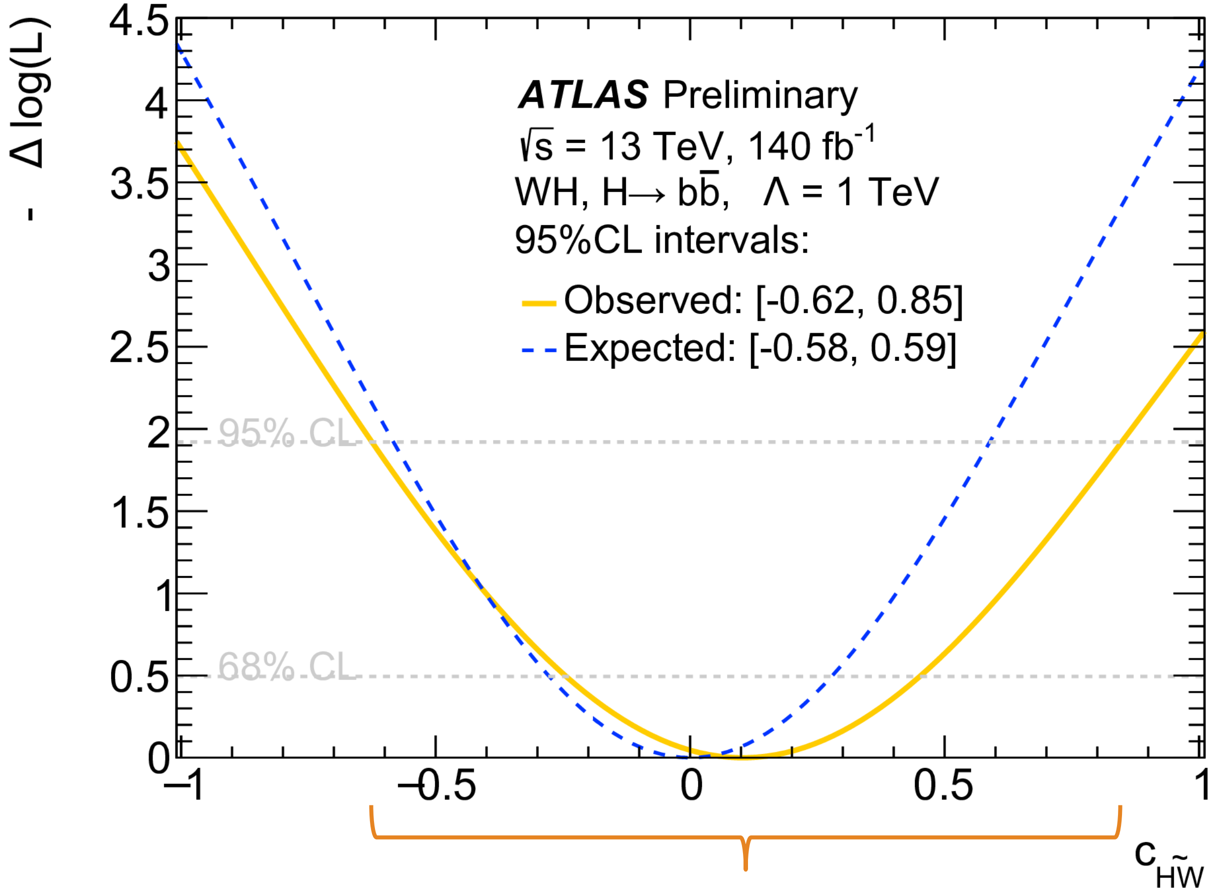

Parameters of interest in the fit:
$c_{H\widetilde{W}}$ + WH signal normalization in each p_T^W bin.

⇒ 95% confidence interval: $c_{H\widetilde{W}} \in [-0.62, 0.85]$
expected: $c_{H\widetilde{W}} \in [-0.58, 0.59]$
(considering only linear order).

See talk by Ricardo Barrue on Wednesday

Summary of ATLAS CP constraints in Run 2

Brand new public plots using 5 full Run 2 analyses (140 fb[-1]): ATL-PHYS-PUB-2025-031

Summary of constraints on $c_{H\tilde{W}}$:

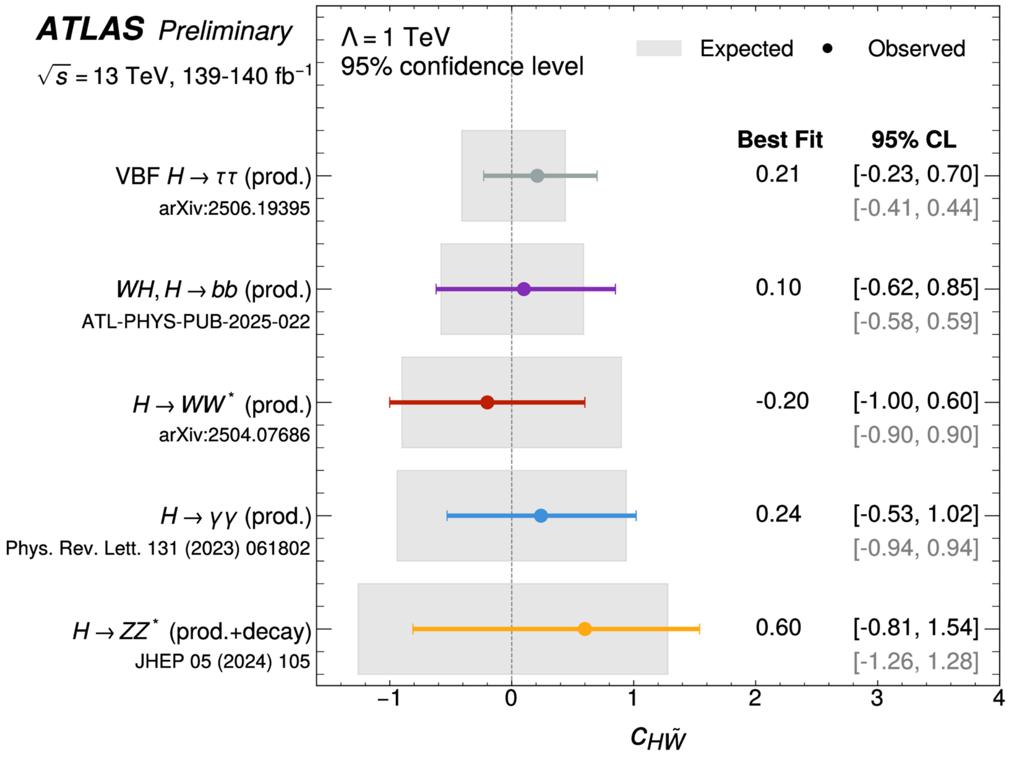

Brand new public plots using 5 full Run 2 analyses (140 fb^{-1}): ATL-PHYS-PUB-2025-031

Summary of constraints on $c_{H\tilde{W}}$:

Covered in this talk

Linear only

Simultaneous fit with other WCs

Linear + quadratic

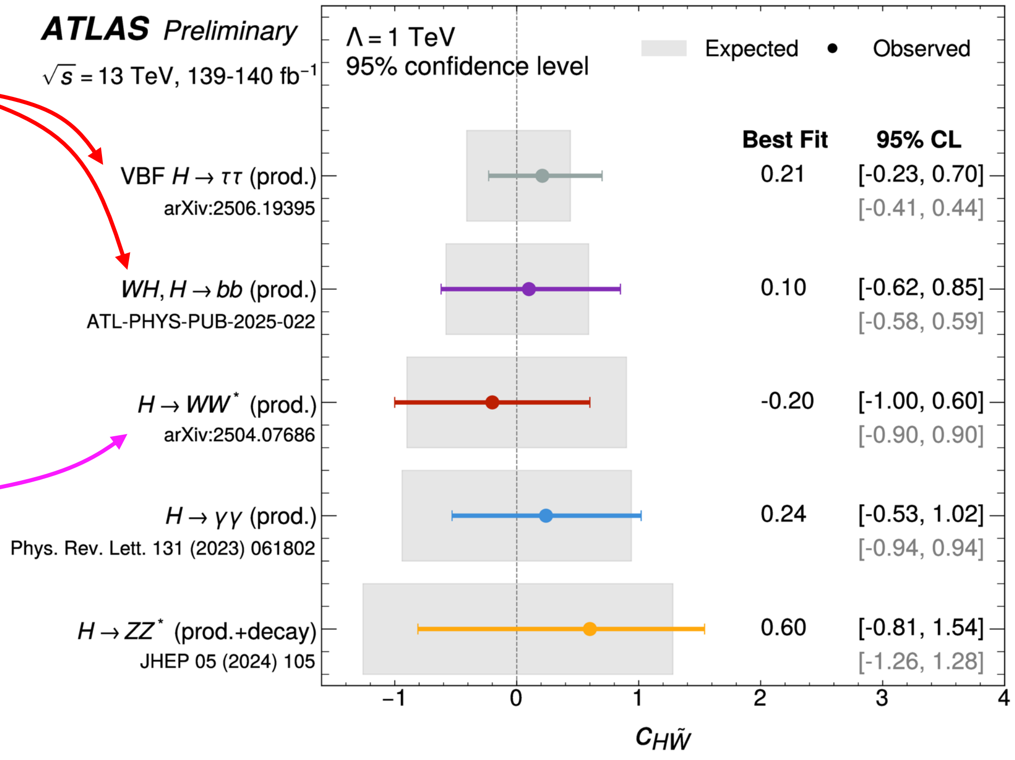

Summary of ATLAS CP constraints in Run 2

Brand new public plots using 5 full Run 2 analyses (140 fb^{-1}): ATL-PHYS-PUB-2025-031

Summary of constraints on $c_{H\tilde{W}}$:

Covered in this talk

Linear only

Simultaneous fit with other WCs

Linear + quadratic

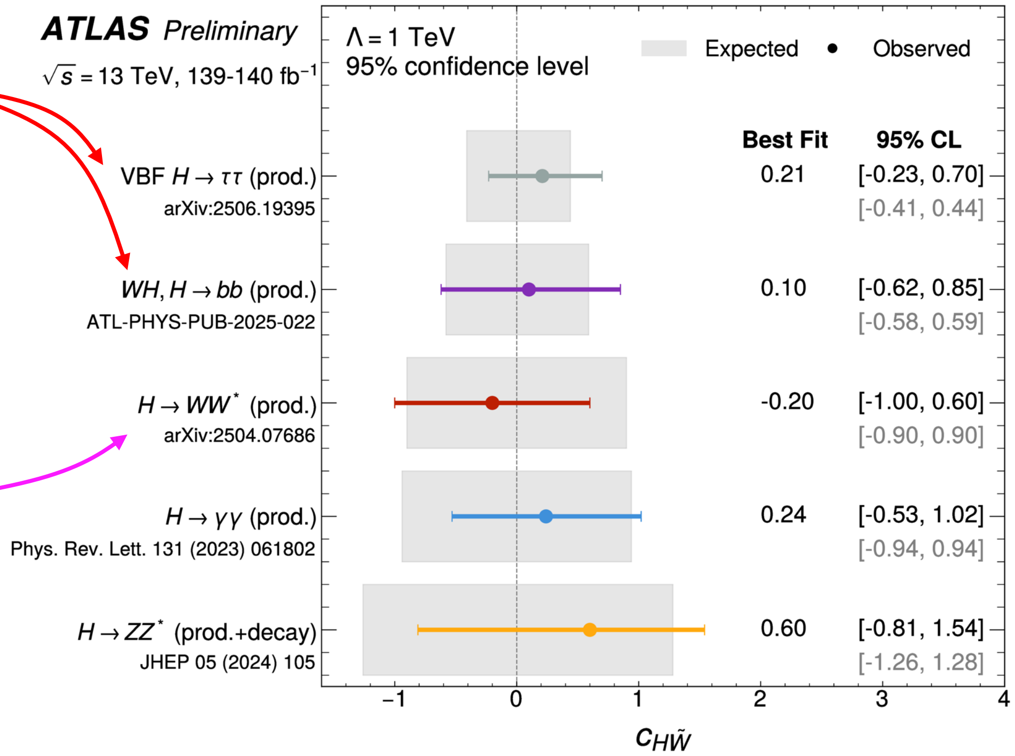

Summary of constraints on Λ:

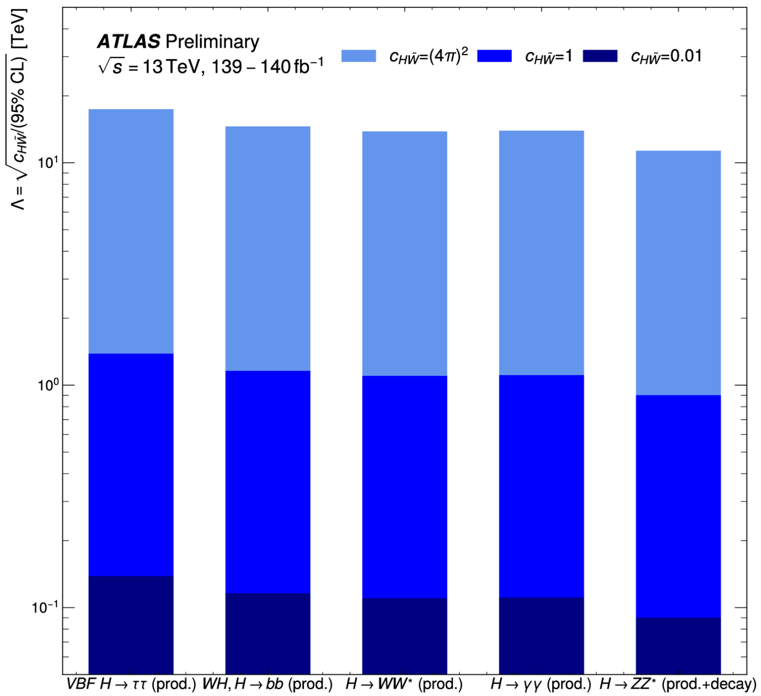

Not an explicit CP measurements but constrains some CP–sensitive operators:

Differential and production mode cross section in $H \to ZZ^* \to 4\ell$ (ATLAS-CONF-2025-002) from April 2025, using 2022-2023 data (56 fb^{-1}):

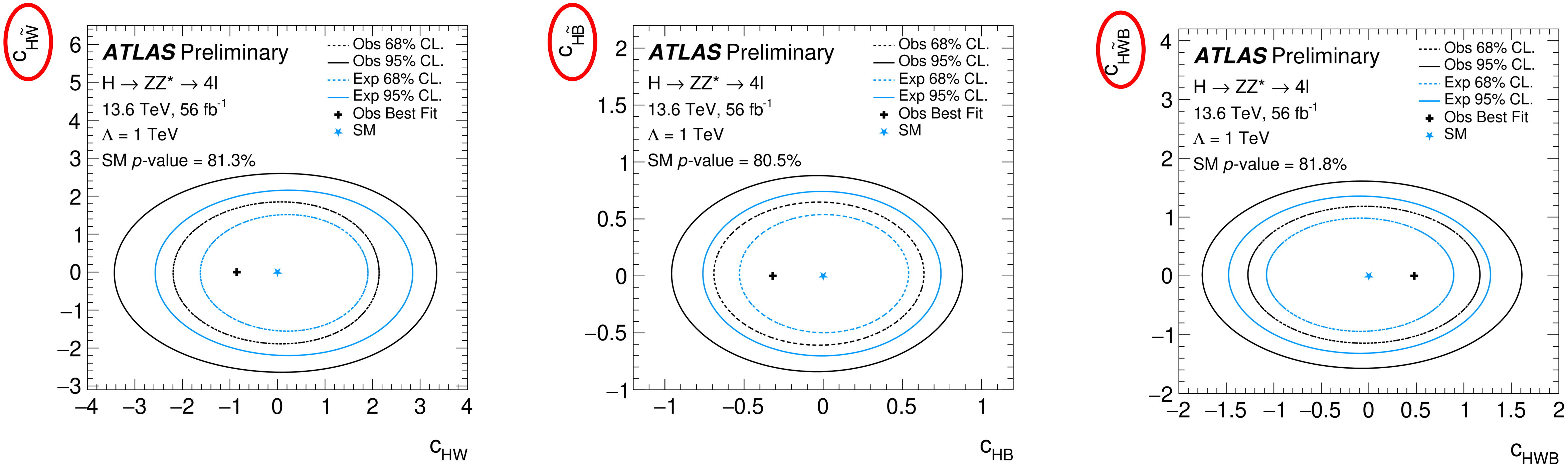

Summary

Summary of results shown in this talk:

	Mass	Width	CP
$H \to ZZ$	$m_H^{ZZ^*} = 124.99 \pm 0.19$ GeV (Run 2)	$\Gamma_H = 4.3^{+2.7}_{-1.9}$ MeV	
$H \to \gamma\gamma$	$m_H^{\gamma\gamma} = 125.17 \pm 0.14$ GeV (Run 2)		
$H \to ZZ + H \to \gamma\gamma$	$m_H = 125.10 \pm 0.11$ GeV (Run 2)		
$H \to WW$		$\Gamma_H = 0.9^{+3.4}_{-0.9}$ MeV	
VBF $H \to \tau\tau$			$\tilde{d} \in [-0.012, 0.034]$ 95% CI $c_{H\tilde{W}} \in [-0.23, 0.70]$ 95% CI (linear only)
$WH, H \to bb$			$c_{H\tilde{W}} \in [-0.62, 0.85]$ 95% CI (linear only)

ATLAS is making full use of the **full Run 2 dataset** and **improved analysis techniques** to reach ever higher sensitivities in Higgs properties!

Backup

Uncertainty breakdown:

Source	Impact [MeV]
Photon energy scale	83
$Z \to e^+e^-$ calibration	59
E_T-dependent electron energy scale	44
$e^{\pm} \to \gamma$ extrapolation	30
Conversion modelling	24
Signal–background interference	26
Resolution	15
Background model	14
Selection of the diphoton production vertex	5
Signal model	1
Total	90

Summary:

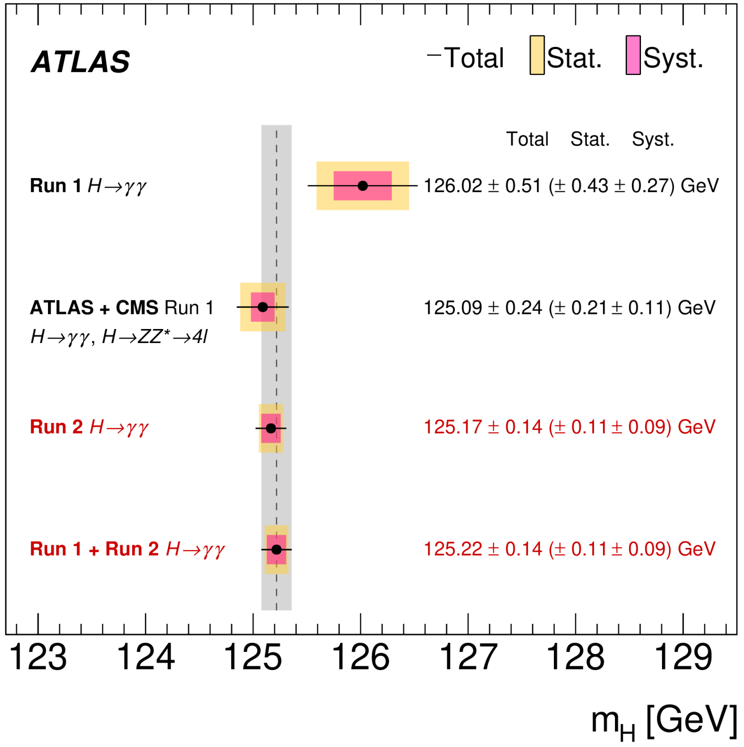

Improvement in photon energy scale:

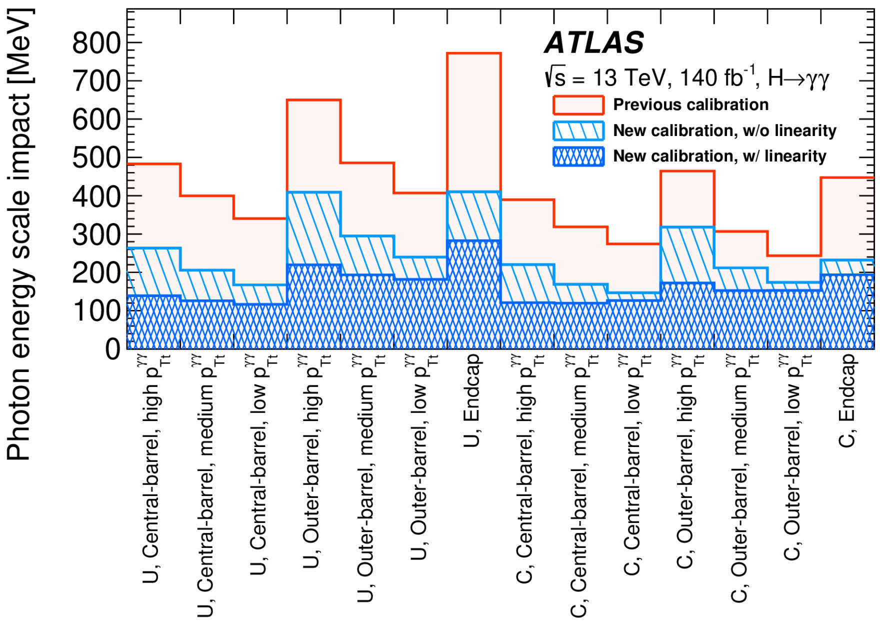

Mass measurement in $H \to ZZ^*$

Pre-fit $m_{4\ell}$ distributions:

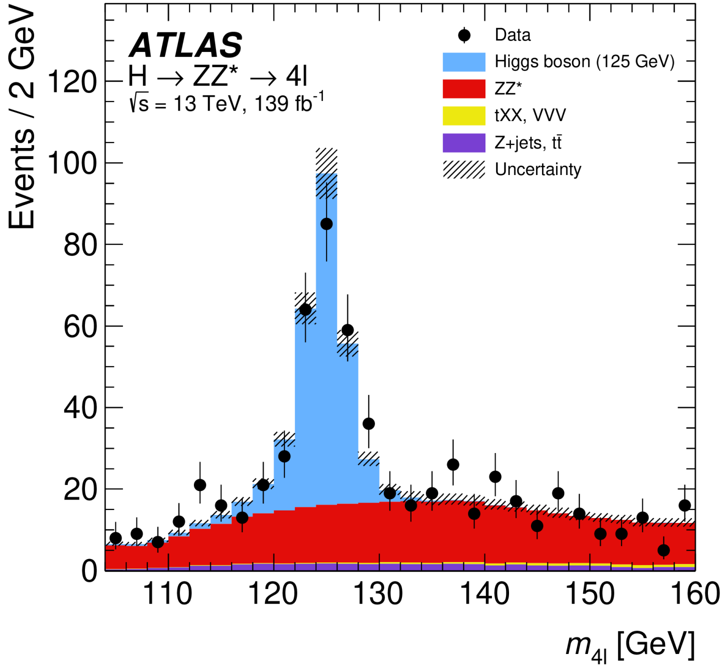

Channel comparison and combination:

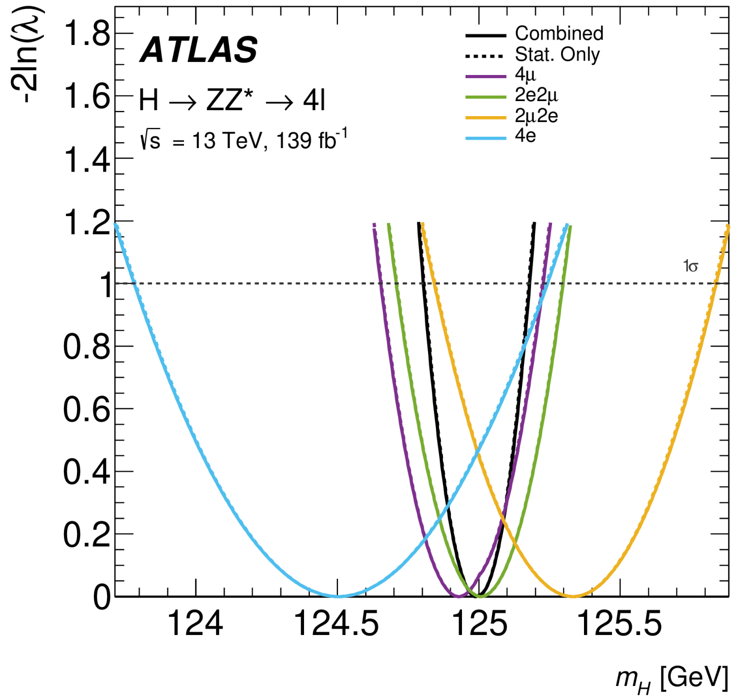

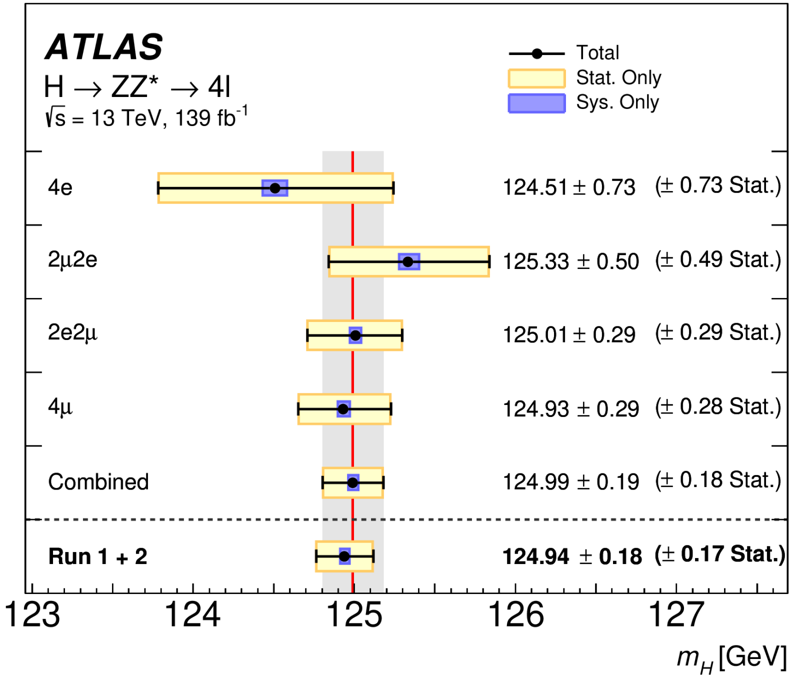

Uncertainty breakdown:

Systematic Uncertainty	Contribution [MeV]
Muon momentum scale	±28
Electron energy scale	±19
Signal-process theory	±14

Mass measurement in $H \to \gamma\gamma$ and $H \to ZZ^*$

Uncertainty breakdown for Run 2 combination:

Source	Systematic uncertainty on m_H [MeV]
e/γ E_T-independent $Z \to ee$ calibration	44
e/γ E_T-dependent electron energy scale	28
$H \to \gamma\gamma$ interference bias	17
e/γ photon lateral shower shape	16
e/γ photon conversion reconstruction	15
e/γ energy resolution	11
$H \to \gamma\gamma$ background modelling	10
Muon momentum scale	8
All other systematic uncertainties	7

Run 1 + 2 combination:

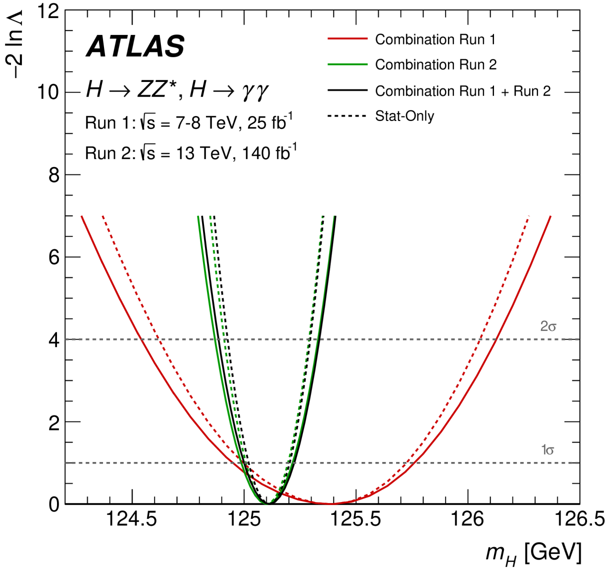

Summary including CMS results:

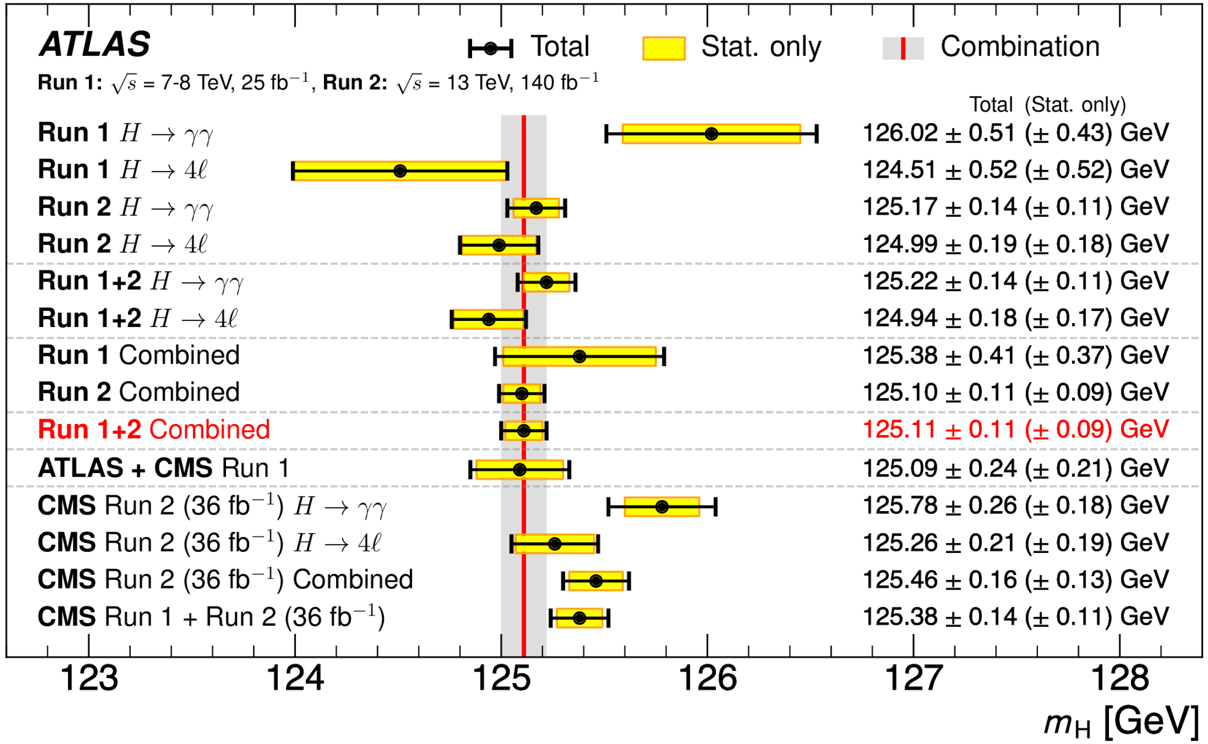

Width measurement in $H \to WW \to \ell\nu\ell\nu$

ggF

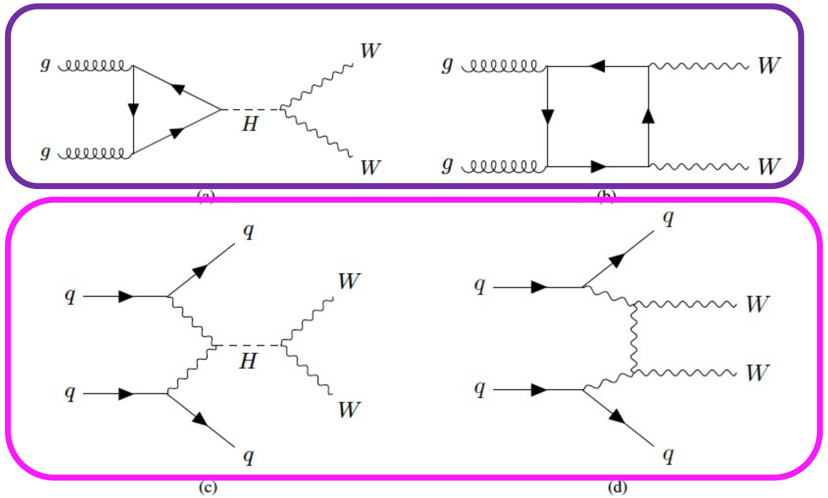

EW

Signal

Interfering background

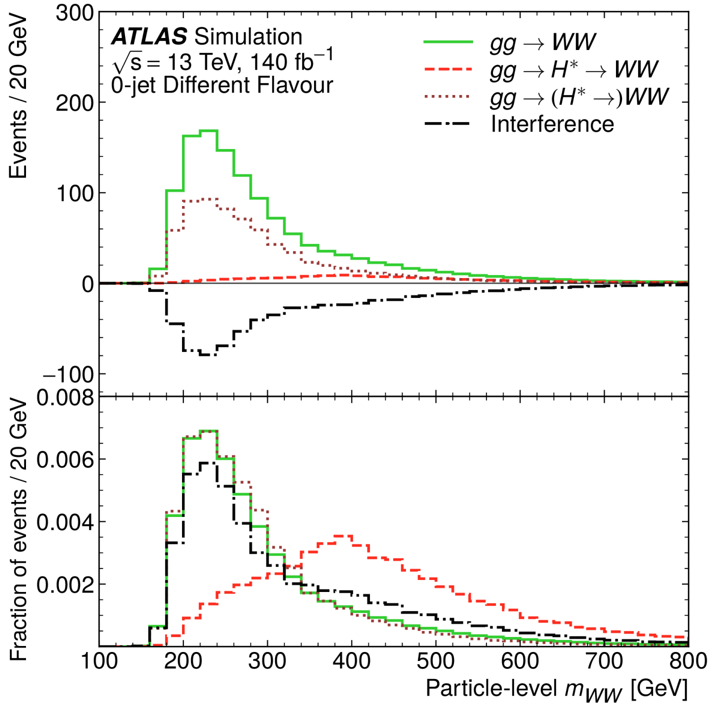

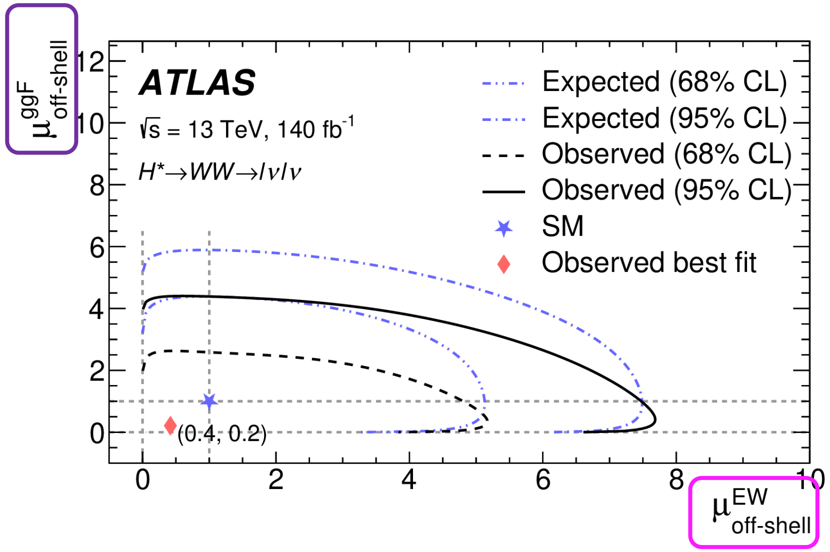

Width measurement in $H \to ZZ \to 4\ell$

ggF

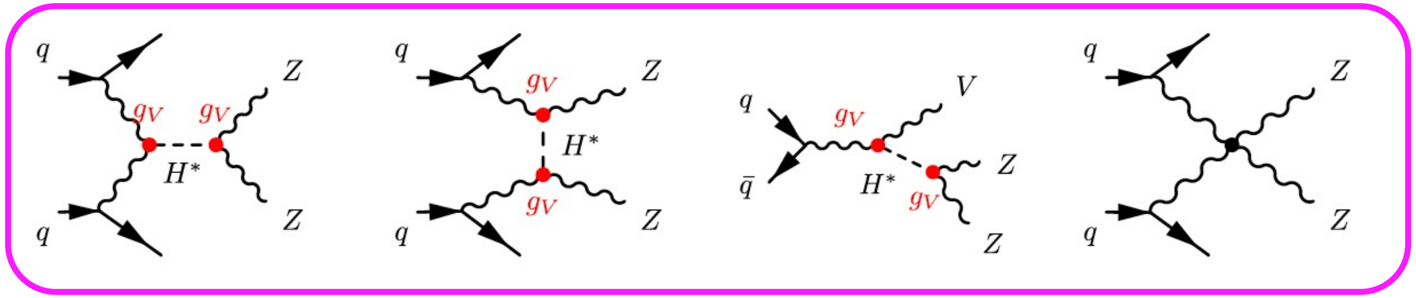

EW

Signal

Interfering background

Probability density equation:

$$p\left(x|\mu^{ggF}_{\text{off-shell}},\mu^{EW}_{\text{off-shell}}\right)=\frac{1}{\nu\left(\mu^{ggF}_{\text{off-shell}},\mu^{EW}_{\text{off-shell}}\right)}\times\Big[\mu^{ggF}_{\text{off-shell}}\nu^{ggF}_{S}p^{ggF}_{S}(x)+\sqrt{\mu^{ggF}_{\text{off-shell}}}\nu^{ggF}_{I}p^{ggF}_{I}(x)+\nu^{ggF}_{B}p^{ggF}_{B}(x)+\mu^{EW}_{\text{off-shell}}\nu^{EW}_{S}p^{EW}_{S}(x)+\sqrt{\mu^{EW}_{\text{off-shell}}}\nu^{EW}_{I}p^{EW}_{I}(x)+\nu^{EW}_{B}p^{EW}_{B}(x)+\nu_{NI}p_{NI}(x)\Big], \quad (3)$$

Likelihood ratio as test statistic: $t_\mu = -2\ln\frac{\lambda\left(\mu,\hat{\hat{\alpha}}(\mu)\right)}{\lambda(\hat{\mu},\hat{\alpha})}$, →

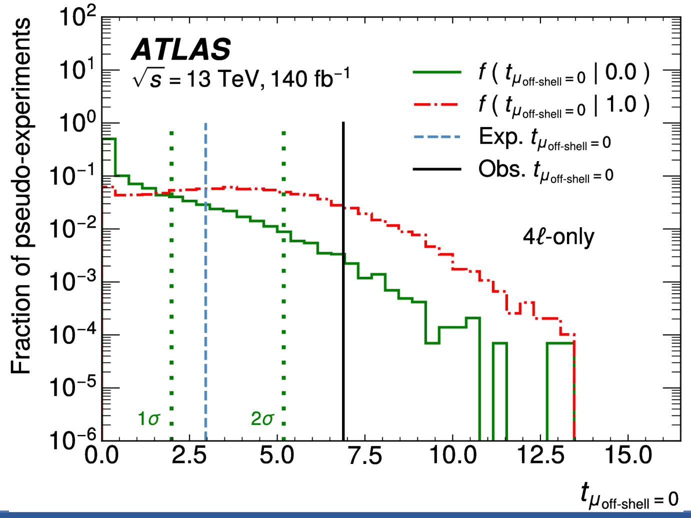

Bonus: width measurement in $t\bar{t}t\bar{t}$

Full Run 2 analysis (140 fb^{-1}) published in February 2025: *Phys. Lett. B* **861** (2025) 139277

Constraint on Higgs boson total width from combination of on-shell Higgs production and $t\bar{t}t\bar{t}$ production:

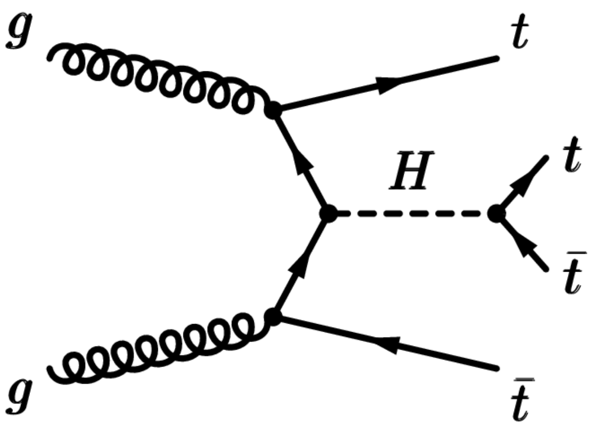

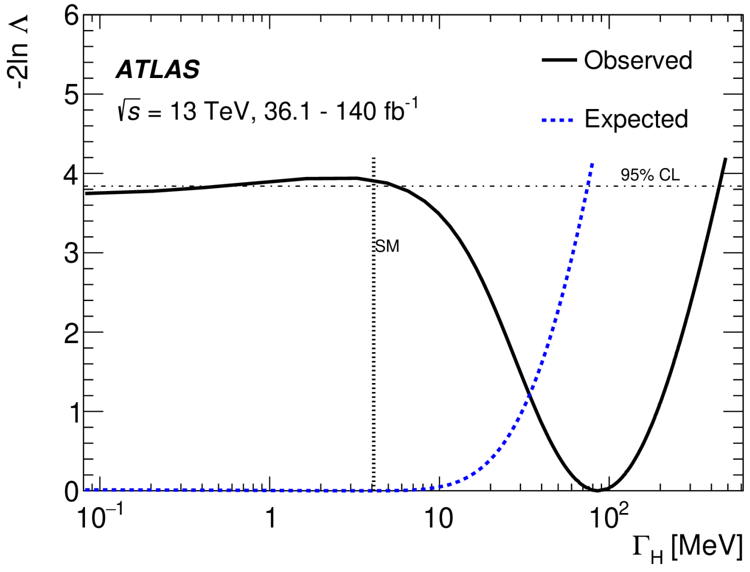

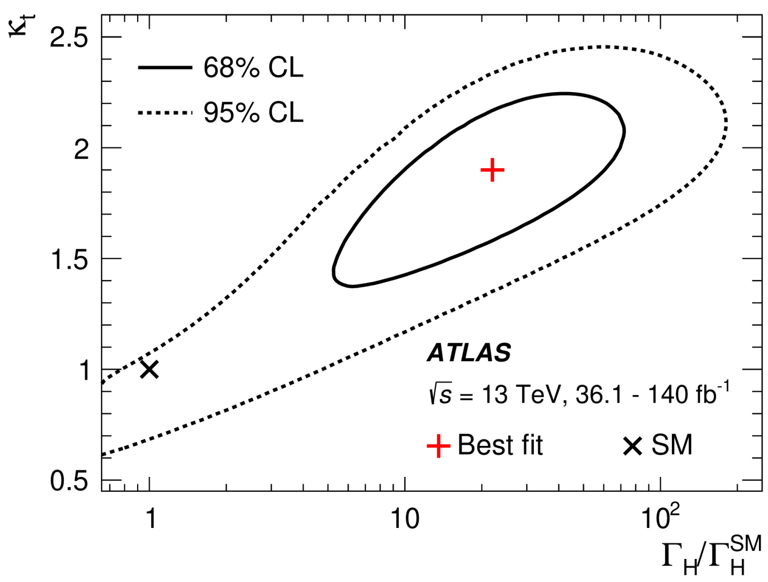

95% CL upper limit: $\Gamma_H \leq 450$ MeV (expected 75 MeV) → 2σ tension with SM, driven by measured $t\bar{t}t\bar{t}$ cross-section, which is 1.8σ above the SM.

See talk by Yangfan Zhang on Tuesday

CP measurement in VBF $H \to \tau\tau$

Sensitive variable: Optimal observable:

$$\mathcal{OO} = \frac{2\mathcal{R}(\mathcal{M}^*_{\text{SM}}\mathcal{M}_{\text{CP-odd}})}{{\mathcal{M}^*_{\text{SM}}}^2}$$

$$2\Re(\mathcal{M}^*_{\text{SM}}\mathcal{M}_{\text{CP-odd}}) = \sum_{i,j,k,l} f_i(x_1)f_j(x_2)2\Re(\mathcal{M}^*_{\text{SM}}\mathcal{M}_{\text{CP-odd}})(ij \to klH)$$

$$|\mathcal{M}_{\text{SM}}|^2 = \sum_{i,j,k,l} f_i(x_1)f_j(x_2)|\mathcal{M}_{\text{SM}}|^2(ij \to klH)\,.$$

Momentum fractions calculated from kinematics of Higgs and VBF jets

Sum over all possible initial and final quark flavors

Matrix Elements are fixed calculations taking quark flavors as inputs.

CP measurement in VBF $H \to \tau\tau$

Uncertainty breakdown:

Systematic source	Uncertainty [%]
Jet/E_T^{miss} reconstruction	± 20
Signal theory	± 15
Background theory	± 11
Normalisation factors	$^{+6.0}_{-5.5}$
Misidentified τ-leptons	± 4.8
τ-leptons reconstruction	± 4.0
Sample size	± 3.0
Leptons reconstruction	± 2.4
Luminosity	± 0.4
Flavour tagging	± 0.3
Embedding	± 0.2
Total systematic uncertainty	± 30
Total statistical uncertainty	± 95

Sensitivity of Optimal Observable compared to alternative variables:

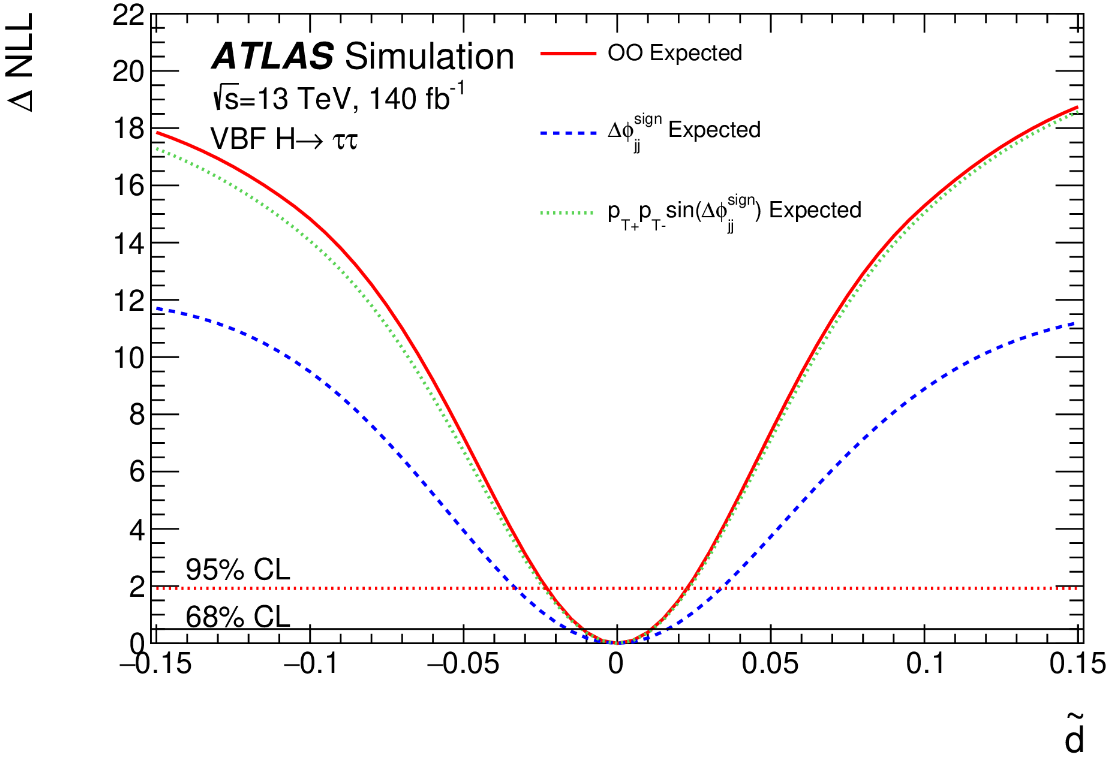

Region definition: